INL/EXT-15-36268

Full Core TREAT Kinetics Demonstration Using Rattlesnake/BISON Coupling Within MAMMOTH

Javier Ortensi, Mark D. DeHart, Frederick N. Gleicher, Yaqi Wang, and Sebastian Schunert.
Idaho National Laboratory

Anthony L. Alberti and Todd S. Palmer
Oregon State University

August 2015

The INL is a U.S. Department of Energy National Laboratory
operated by Battelle Energy Alliance

Idaho National Laboratory

INL/EXT-15-36268

Full Core TREAT Kinetics Demonstration Using Rattlesnake/BISON Coupling Within MAMMOTH

**Javier Ortensi, Mark D. DeHart, Frederick N. Gleicher,
Yaqi Wang, and Sebastian Schunert
Idaho National Laboratory**

**Anthony L. Alberti and Todd S. Palmer
Oregon State University**

August 2015

**Idaho National Laboratory
Reactor Physics Analysis and Design Dept.
Idaho Falls, Idaho 83415**

http://www.inl.gov

**Prepared for the
U.S. Department of Energy
Office of Nuclear Energy
Under DOE Idaho Operations Office
Contract DE-AC07-05ID14517**

Full Core TREAT Kinetics Demonstration Using Rattlesnake/BISON Coupling Within MAMMOTH

Javier Ortensi, Mark D. DeHart, Frederick N. Gleicher, and Yaqi Wang
Idaho National Laboratory

Anthony L. Alberti and Todd S. Palmer
Oregon State University

ABSTRACT

This report summarizes key aspects of research in evaluation of modeling needs for TREAT transient simulation. Using an experimental TREAT critical measurement and a transient for a small, simplified core, Rattlesnake and MAMMOTH simulations are performed building from simple infinite media to a full core model. Cross section processing methods are evaluated, various homogenization approaches are assessed and the neutronic behavior of the core studied to determine key modeling aspects. The simulation of the minimum critical core with the diffusion solver shows very good agreement with the reference Monte Carlo simulation and the experiment. The full core transient simulation with thermal feedback shows a significantly lower power peak compared to the documented experimental measurement, which is not unexpected in the early stages of model development. For this reason, a sensitivity analysis to the adiabatic model and the magnitude of the reactivity insertion are included.

1.0 INTRODUCTION

Operating from February 1959 until April 1994, the Transient Reactor Test Facility (TREAT) at Idaho National Laboratory (INL) was specifically built to conduct transient reactor tests where the test material is subjected to neutron pulses that can simulate conditions ranging from mild upsets to severe reactor accidents. The reactor was constructed to test fast reactor fuels, but has also been used for light water reactor fuel testing as well as other exotic special purpose fuels. [1, 2]

TREAT is an air-cooled, thermal-spectrum test facility designed to evaluate reactor fuels and structural materials under simulated nuclear excursions and transient power/cooling mismatch situations in a nuclear reactor. [3] Such testing involves placing fuel or material into the TREAT core and subjecting it to short bursts of intense, high-power neutron radiation. After the experiment is completed, the fuel or material is analyzed to determine the effects of the power burst. The resulting information is then used to guide the development and improvement of advanced nuclear fuel designs, and to validate computer models of fuel and core behavior required for U.S. Nuclear Regulatory Commission (NRC) evaluation of nuclear power reactor design and safety evaluations. [2]

The U.S. Department of Energy Office of Nuclear Energy (DOE/NE) is preparing to resume operation of the Transient Reactor Test Facility at the Idaho National Laboratory, more commonly known as TREAT.

The pulsed reactor, built in 1959, has not operated since 1994, at which time it was placed in a standby mode. It is anticipated that the facility will become full operational around 2018.
Historical methods used for pre-transient calculations were very approximate low order methods that required a number of reduced and full power tests to obtain correction factors to improve the prediction of the full power transient prior to the test itself. The use of modern modeling and simulation (M&S) tools, capturing the multi-physics nature of TREAT operation and experimentation, has the potential for reducing the number of low and high power calibration tests needed prior to full power operations for a transient experiment. This would result in significant operational efficiency with corresponding cost savings, and would also lay the groundwork for improved fidelity in experiment design. Hence, INL is engaged in efforts to develop full multi-physics modeling capabilities to predict core transient behavior (power excursions with thermal feedback) and its coupling with experimental configurations, supported by the Nuclear Energy Advanced Modeling and Simulation (NEAMS) program, within DOE/NE.

Reduction of the number of TREAT calibration tests and the corresponding development of a three-dimensional coupled modeling and simulation (M&S) capability to model reactivity insertion accident (RIA) behavior of fuel experiments in TREAT will result in major facility cost reduction and higher experimental capacity. This M&S capability will enable improved core operation as well as design and analysis of TREAT experiments. The ultimate goal of this work is thus to provide a validated M&S platform to accurately describe the integrated TREAT system behavior (reactor, experiment test train, and experiment). This platform will support test train design and definition of reactor operating parameters without conducting the traditional number of low and high power experiment calibration runs. In the first year of this project, work has been focused on development and testing of single element (infinite lattice) and full core models, with which to conduct convergence studies (grid, time step, energy groups, etc.); addition of thermal properties for TREAT materials; demonstration of successful coupling between neutronic and temperature feedback calculations and estimations of total core power during a transient with thermal feedback to demonstrate full core kinetics capabilities. The latter is the subject of this report, while the other work listed is described in Refs. 4 and 5.

2.0 CORE MODELING APPROACH

The TREAT core provided a number of modeling challenges that are best addressed in a multi-physics simulation. Close coupling between neutron reaction rates and local temperature for a transient that lasts only a few seconds is critical to ensure that the time-dependent energy release is accurately predicted. The following subsections describe the general approach taken at INL to be able to accurately simulate TREAT transient behavior.

2.1 Multi-Physics Simulations

INL has developed high-fidelity, tightly coupled multi-physics modeling under the award-winning [6] Multi-physics Object Oriented Simulation Environment (MOOSE) framework [7]. MOOSE enables development of simulation tools in a fraction of the time previously required. A simulation effort requiring a team of ten people working for five years can be completed by three people in one year. The simplicity has bred 40 different MOOSE-based modeling applications. The rapidly growing MOOSE user community spans nuclear engineering, material science and geology and includes 45 domestic or foreign labs, universities and companies.

The MOOSE framework consists of several consistently designed, pluggable interfaces that scientists and engineers use to solve domain-specific problems. Internally, MOOSE utilizes the finite element method mathematical modeling technique due to its generality and wide applicability. In this work, the MOOSE-based transport solver Rattlesnake was used for neutron transport calculations and reactor physics tool MAMMOTH was employed to perform coupled calculations.

2.2 MAMMOTH Reactor Physics

The reactor physics application MAMMOTH has been designed and implemented using the MOOSE environment [8]. MAMMOTH allows the coupling of a number of other MOOSE-based sub-applications including: Rattlesnake [9] for neutron transport, RELAP-7 [10] for low-resolution thermal-fluids, and BISON [11] for fuel performance analyses. In general MAMMOTH has great flexibility to solve complex reactor multi-physics problems. One approach is by solving a large system of interlinked nonlinear equations on the same mesh. These equations can be simultaneously solved with the Jacobian-Free Newton-Krylov (JFNK) method [7]. However, because of needs in some problems for solutions on varying time scales, implicit coupling is not optimal. Hence, a split operator approach is available where each sub-application solves its individual physics and has a coincident mesh with the other application [8,12]. Data is then shared between each sub-application coupling them using the MOOSE MultiApp system [8,13]. For this form of coupling an additional outer iteration and time substeps can be applied to make the physics more consistent. The MOOSE framework provides the necessary flexibility to perform multi-scale modeling where necessary, which will be imperative in experiment analysis and design. The general long-term technical objective of the currently funded MAMMOTH project in support of TREAT is to develop a set of high-resolution reactor physics and fuels performance models that can accurately predict the transient behavior of an in-core experiment as driven by a reactor transient. Current MAMMOTH development efforts are focused on capabilities that can be used in simulation of coupled neutron and thermal physics phenomena and scoping design and post-test experiment analysis for TREAT [4,5].

A key feature of MOOSE-based applications is that a particular tool (in this case MAMMOTH) is compiled as a single executable code containing executable libraries for each component sub-application. In other words, within the MAMMOTH executable are embedded the full set of capabilities of BISON, Rattlesnake, RELAP-7 and MOOSE. Communications between packages is done in-core using shared memory managed by MOOSE algorithms. MAMMOTH also inherits the advances in each of the applications and enforces code compatibility for all applications. In the near future, additional sub-applications will be added to MAMMOTH to expand its range of capabilities. Although studies have been completed [14], this form of implicitly and explicitly coupled multi-physics capability existing in one code with a unified data/communications/solution structure is not known to exist for traditional reactor analysis applications [15].

2.3 Problem Description

The primary goal in TREAT transient simulation in the first year of this project has been to demonstrate and ultimately validate MAMMOTH power transient simulations with coupled transport/heat transfer calculations using both Rattlesnake and BISON within MAMMOTH. Accurate representation of the shape and magnitude of the transient pulse will be essential to properly simulate the tightly coupled physics phenomena anticipated in experiment test rigs. The work included in this report describes recently

completed calculations of a simple TREAT transient with thermal feedback. Efforts were made to capture all-important neutronic dimensions of a documented core configuration [16] with material-appropriate thermal properties, and to simulate the reactivity increase for a documented transient test; however, the work described herein does not necessarily rise to the level of benchmark quality. At present, the focus of this work is to begin to understand the dynamics of transient behavior with temperature feedback and to identify key modeling requirements needed to minimize error.

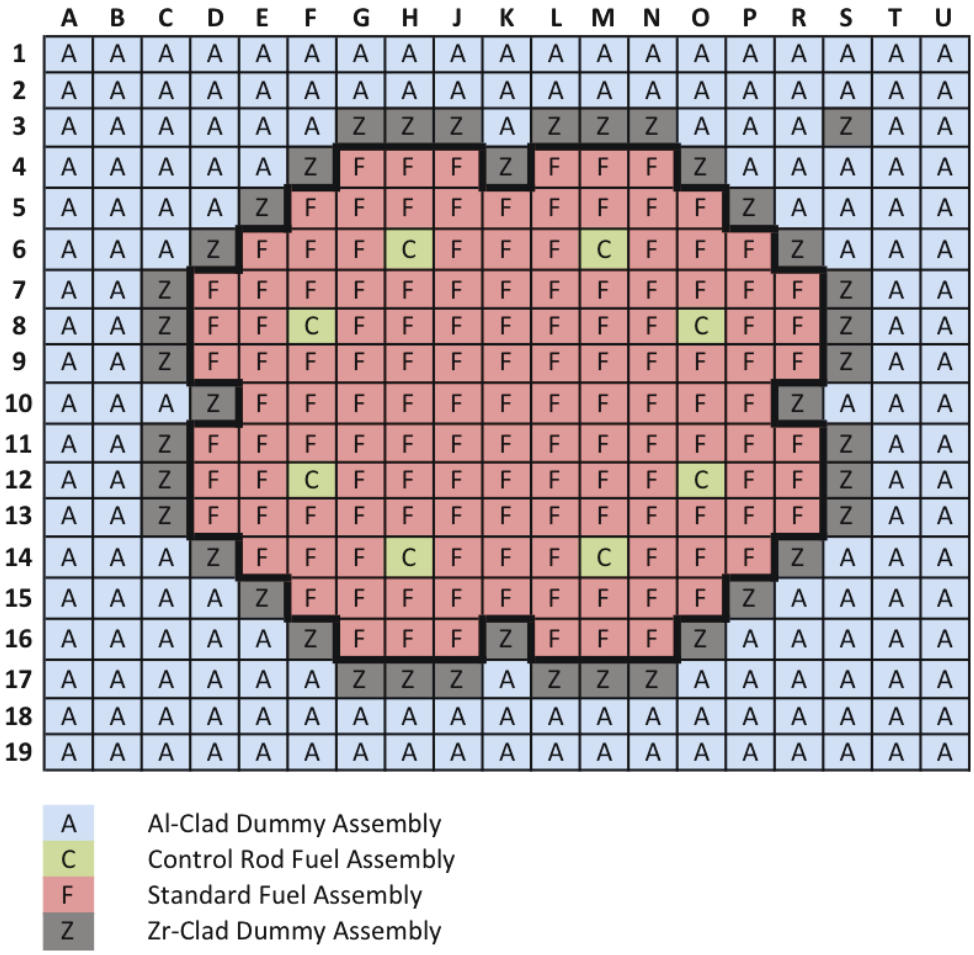

Fig. 2.1. 138-element minimum critical core configuration [16].

For this work, two configurations have been evaluated. The 138-element minimum critical core configuration [16, 17] was the one of the first critical states measured within TREAT, and serves as a good starting point for evaluation of MAMMOTH cross section and meshing data to match the critical state. A core face-map of the minimum critical configuration is shown in Fig. 2.1. Note that this core was intended only for critical measurements and no transients were performed. Thus, for transient simulations, the 159-element "small core" configuration of transient 15 (from Table XIII of Ref. 17) was selected as a starting point based on the nature of the experiment and available data. This core configuration is shown in Fig. 2.2, and is a relatively simple configuration with no viewing slot. Note that for this model the locations for the thermocouple fuel elements have been replaced with standard fuel elements. Also, the source location has been replaced with a zirconium clad dummy element.

Transient 15 of the “small core” configuration was a temperature limited transient experiment conducted with a total reactivity insertion of 1.55% Δk ($2.16). Following the transient the reactor was returned to critical to find the total reactivity change resulting from the transient; from this it was determined that the total reactivity in the core from temperature feedback was -2.31% (-$3.22). This core was selected due to the simplicity of the configuration and minimal control rod locations; however, detailed control rod positioning data were not provided, so approximations were employed.

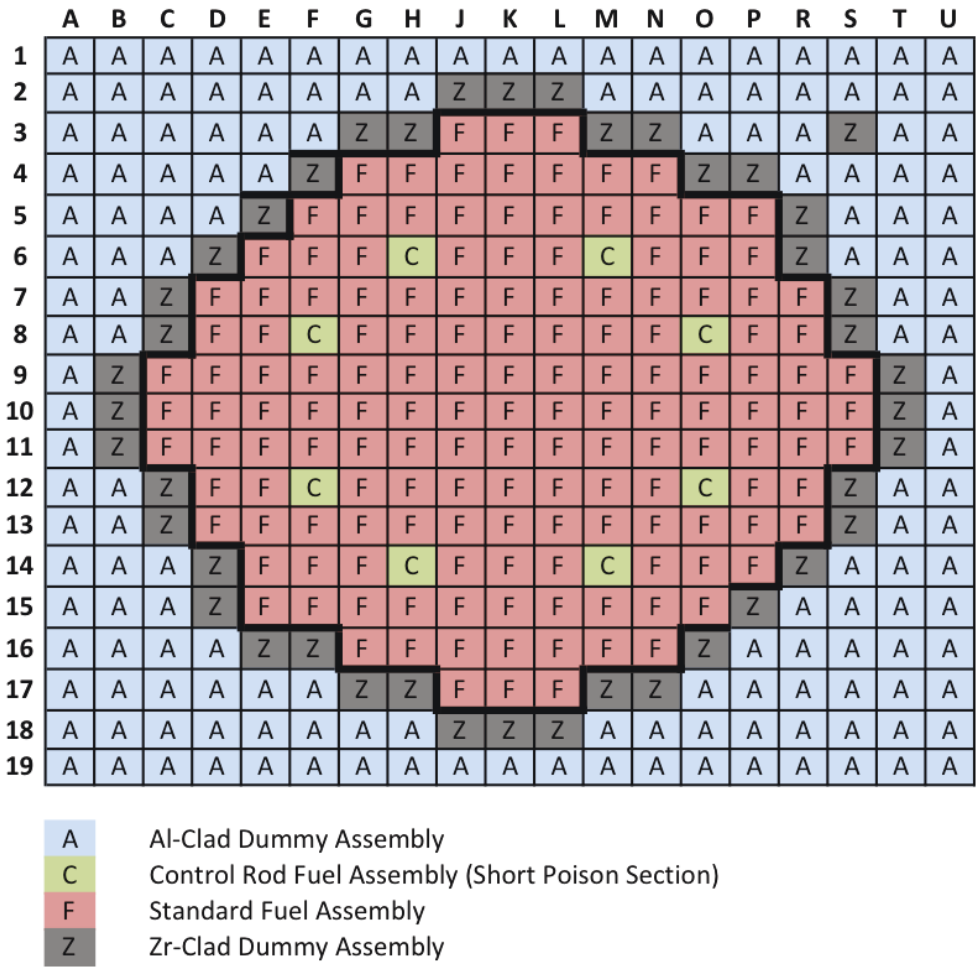

Fig. 2.2. 159-element small core configuration of calibration transient 15 [17].

3.0 APPROACH

This section documents the development of a MAMMOTH model, which essentially required three necessary steps: 1) the preparation of data, 2) the development of an analysis mesh, and 3) assemblage of the MAMMOTH model. These tasks were not completely sequential in nature and tended to evolve as the analysts improved the various parts of the final model. The generation of the cross section data and meshing went hand-in-hand since the cross sections were homogenized over several materials in order to simplify the mesh and, thus, the cost of the simulation. It was also determined that the model initially assembled could not be solved with certain transport solvers available in Rattlesnake. For example, the

second order self-adjoint formulations of the spherical harmonics solver or the discrete ordinates calculation of the angular flux were known to experience numerical convergence difficulties in near-void regions. Such difficulties were be addressed by appropriate homogenization of lower density regions with adjacent structure (and also let to code updates to address these shortcomings). For this reason, both the meshing and data preparation are dependent on the solver used. Section 3.1 discusses the preparation of the neutron cross section, delayed neutron data, and the basic thermo-physical properties for the feedback models. This is followed by a description of the mesh generation for the various elements and the full core configurations in Section 3.2. Finally, the description of the MAMMOTH models used in these calculations is provided in Section 3.3.

3.1 Model Data

Because this is a coupled calculation, both physics (cross sections and kinetics parameters) and thermal (conductivity, heat capacity) are required. The following sections describe sources of data and any assumptions made.

3.1.1 Cross Section and Delayed Neutron Data Preparation

The majority of cross sections and delayed neutron data used this report were prepared with Serpent 2 [18] with ENDF/B-VII.1-based cross sections. Serpent 2 is a three-dimensional continuous-energy Monte Carlo reactor physics code developed at VTT Technical Research Centre of Finland. Serpent 2 has been selected for this project because it offers spatial homogenization and multi-group constant generation for deterministic reactor simulations from a Monte Carlo simulation. At the same time Serpent 2 provides a detailed reference calculation without energy, angular, or spatial discretization error. The cross sections for near-void regions were initially developed with DRAGON-5 [19], since Serpent 2 was not able to calculate appropriate diffusion coefficients for these regions with the current geometry. In order to better capture the streaming that takes place in the air channel with diffusion, the diffusion coefficient in this region was artificially increased by a factor of 2.5 to 4. A detailed description of the cross section preparation tasks for this work is included in a separate report [20].

For initial studies, cross sections and delayed neutron data were prepared and tabulated for a fully homogenized model comprised only of an infinite medium of TREAT fuel (actually, a finite volume with reflective boundary conditions). For this cross section set the tabulation included a variation in the boron concentration for the fuel mixture. This was followed with the preparation of a data tabulation for the standard TREAT element model with reflective boundary conditions in the x-y plane and void boundary conditions in the above and below the top and bottom element fittings (i.e., an infinite x-y lattice of fuel elements). The standard element tabulation included fuel temperatures from 300 to 800 K and two boron concentrations for the fuel region. Finally, data were tabulated for the two full core configurations: 1) a fuel temperature tabulation for the minimum critical core and 2) a fuel temperature and control rod boron concentration tabulation for the 159-element core. Note that the cross sections developed for the various elements in the full core configuration are based on the average element of the same type in the core. In the future this can be improved by using a variety of standard elements based on their position within the core (i.e., near reflectors, CR elements, experiment, etc.).

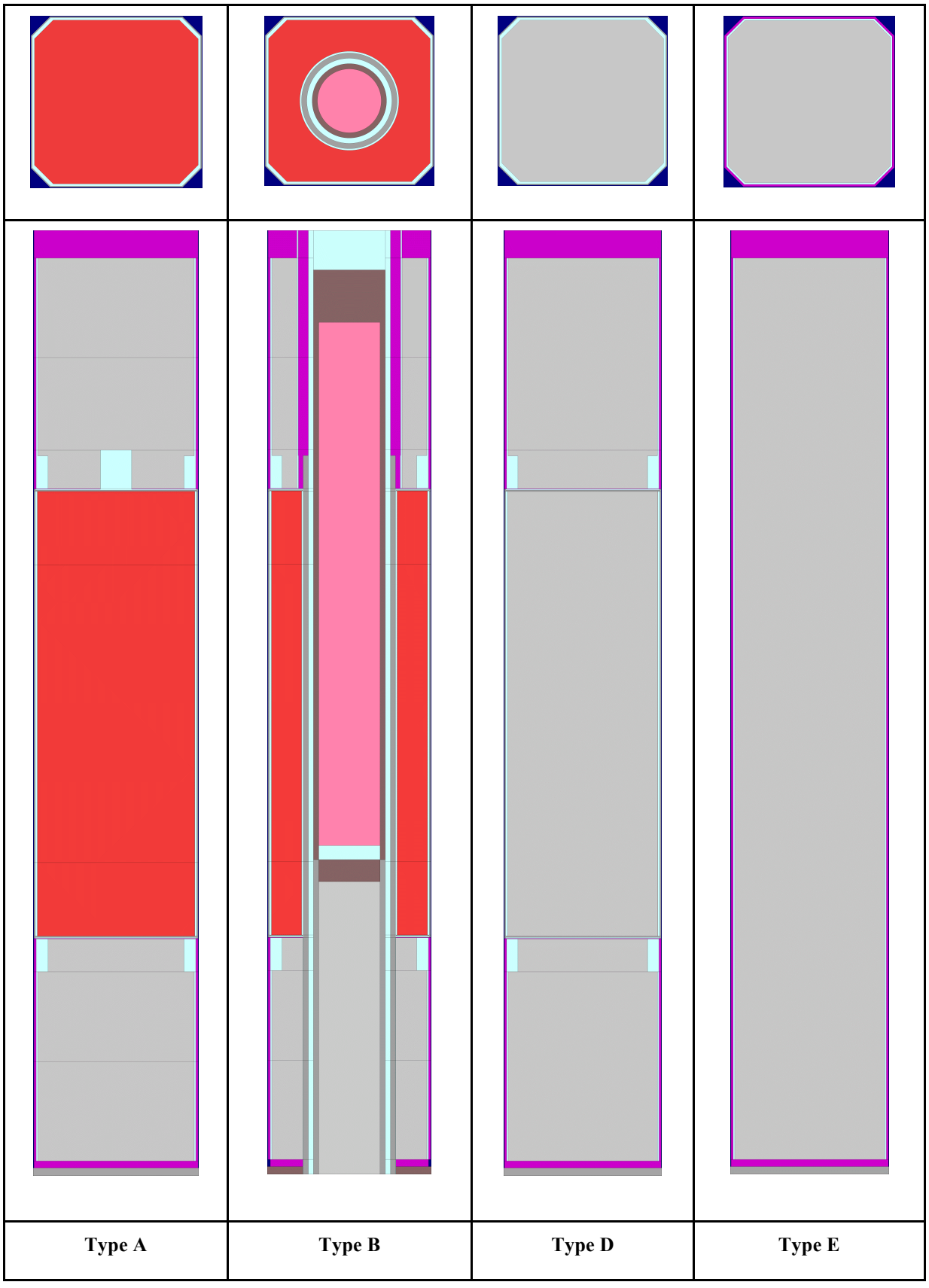

Fig. 3.1. Serpent 2 models of the TREAT elements (not to scale)

A number of energy group structures were briefly studied [20] and an 11 energy group structure based on an HTR 26 group structure was selected. The TREAT elements used in this analysis include: A) standard fuel, B) control rod fuel, D) zircaloy-clad dummy, and E) aluminum-clad dummy. The TREAT Type C slotted element is used in cores with an access slot to the hodoscope and is not part of this work. Figure 3.1 includes the geometric plots from the various Serpent 2 element models.

Over the course of this work it was determined that a significant challenge in the modeling of TREAT is the streaming of neutrons in the air channel, which comprises the region outside the cladding, i.e., the inter-element gap and corner air channels. Modeling of the air channel introduces substantial problems for the diffusion solver as well as the second order formulations of the transport equation. In order to alleviate some of these problems, several radial homogenization strategies were developed [20]. This report only includes results from the following:

- *full* -- all of the radial regions homogenized together.
- *full with channels* -- full homogenization with separate air cooling channels and inter-element gaps.
- *heterogeneous* – graphite regions are homogenized with the gap up to the fuel outer dimension. The air gap, clads, and air channel are treated explicitly.

For the standard and control rod fuel elements, the following **axial** cross section homogenization regions have been defined:

1. Homogenized steel base with bottom aluminum fitting.
2. Octagonal graphite regions 1 and 2 for both top and bottom reflectors are based on spectral analysis at 300 K. In region 1, which is located further away from the active core, the neutron spectrum changes more rapidly due to leakage effects. Region 2 exhibits a milder neutron spectrum gradient.
3. The bottom square graphite.
4. The axial interface region is comprised of the top or bottom aluminum clad from the reflector can, the top or bottom zircaloy clad from the fuel can, the zircaloy spacer and the corresponding gap in the axial interface region.
5. The location of fuel regions 1 and 2 are based on spectral analysis at 300K. Region 1 corresponds to the region where the neutron spectrum changes more rapidly due the reflector effects, whereas region 2 is a constant spectrum region.
6. Top square graphite (with outgas tube hole) and octagonal graphite (with outgas tube hole) are homogenized together.
7. Top aluminum fitting.

3.1.2 Thermophysical Data

The density and heat capacity of the graphite-urania fuel from the TREAT Design Summary Report [21], Appendix B, are shown in Table 3.1. The heat capacity was converted to J/g/K.

Table 3.1. Thermophysical Properties of Graphite-Urania Fuel

Density [g/cm^3]	ρ= 1.72
Conductivity [W/cm/K]	$k = 2.92956\text{x}10^{-1} - 2.55769\text{x}10^{-4}\,T + 1.79589\text{x}10^{-7}\,T^2 - 4.72130\text{x}10^{-11}\,T^3$
Heat capacity [J/g/K]	$C_p = -2.21720\text{x}10^{-2} + 7.02073\text{x}10^{-4}\,T - 3.01660\text{x}10^{-7}\,T^2$

The current adiabatic model uses a single value for the energy to temperature conversion coefficient; the value used in this study is

$$\epsilon = \frac{1}{\rho Cp} = 2.7634 \text{ K-cm}^3\text{/J} \qquad (3.1)$$

3.2 Model Mesh

Geometric models and their corresponding meshes were created with CUBIT, a full featured mesh generation toolkit designed by Sandia National Laboratory. CUBIT has been developed to create two- and three-dimensional finite element meshes and utilizes either unstructured or structured mesh elements. CUBIT also has the capability to generate mixed element meshes [22]. Finite element models are typically prepared through the EXODUS-II format. Using this format, boundary conditions and material properties are applied via surface element based side-sets and blocks. Side-sets are used to apply boundary conditions to sides of elements, such as faces of hexes or edges of quads [23]. Blocks allow for users to group specific volumes together based on material properties. A powerful aspect of CUBIT is the ability to interface with Python. This interface provides a mechanism through which the CUBIT bodies may be created and stored. It also provides an object oriented structure that gives users the ability to easily manipulate and query CUBIT bodies. Because of these capabilities, CUBIT is often used as the mesh generation tool for MAMMOTH applications.

Models analyzed in this report were created using a modularized format of Python scripts. The following general module format was used: 1) main input; 2) geometry building functions; 3) advanced CUBIT functions; 4) main executioner. The main input is used to store model specifications such as mesh refinement, geometrical dimensions, and domain identifiers for material property and boundary condition applications. Due to the similarity of each of the elements in the TREAT core, the general geometrical shapes used in the models were able to be created via general functions. These functions were stored as a separate module script for ease of editing and modifying models. The advanced function module allows users to call predefined functions that query and manipulate geometrical objects. The executioner, is the main file that links the other three modules and does the heavy lifting of creating, modifying, and meshing the models.

3.3 MAMMOTH Models

Since there is no prominent deformation by the reactor fuel, such as in LWR fuel during operation, the thermal mesh may be assumed to be the same as the neutronic mesh for either the element or reactor. This allows both loose or weak coupling and fully implicit or strong coupling to be applied for feedback calculations.

3.3.1 Thermal model

The transient studies included in this report use a simple adiabatic model (no heat flow through the boundaries) for the fuel temperature field solution during the transient. The adiabatic model has the form:

$$\frac{\partial T(r,t)}{\partial t} = \epsilon\, \kappa(T(r),t)\Sigma_f(T(r),t)\psi(T(r),t) \qquad (3.2)$$

where

ψ is the scalar flux [n/cm^2-s]

Σ_f is the fission cross section [cm^{-1}]

κ is the energy release per fission [J/fission]

$\epsilon = \frac{1}{\rho Cp}$

3.3.2 Homogeneous Medium Model

The homogeneous medium model is essentially a homogeneous 3-D volume with reflective boundary conditions. Both a steady state and a transient case were used to determine the consistency of the various Rattlesnake solutions available.

3.3.3 Standard Element Model

A number of standard element models were built for MAMMOTH based on the various radial homogenization schemes from the cross section task. Axially the standard element contains the same regions that were defined in the Serpent 2 model. Reflective boundary conditions were imposed in the x-y plane and void boundary conditions on both axial ends. A set of steady state calculations at different temperatures is used to determine the power distribution, temperature coefficients, reaction rates, and leakage rates. The majority of the transport solutions were based on diffusion theory. In the *full with channels* (Fig. 3.2) and *heterogenous* (Fig. 3.3) models the diffusion coefficients for the air channel were artificially increased in order to increase the neutron streaming in the air channel away from the active core region.

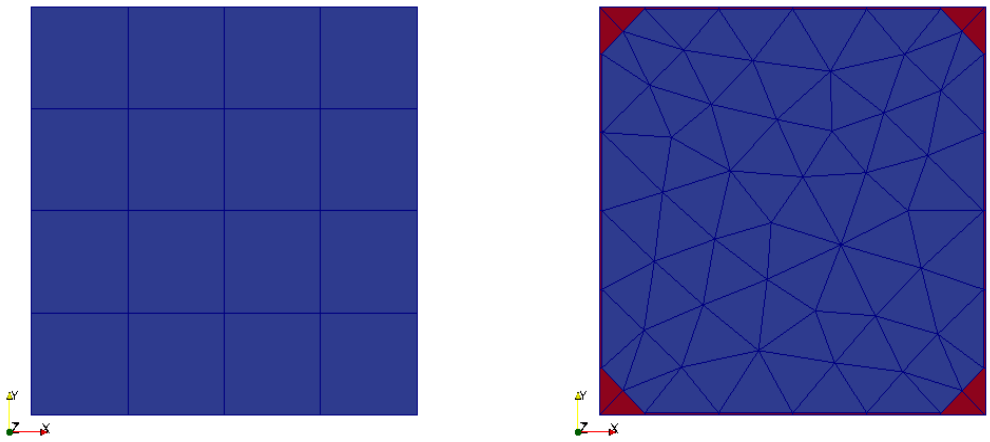

Fig. 3.2: Top down view of the mesh for homogenization *full* and *full with channel*.

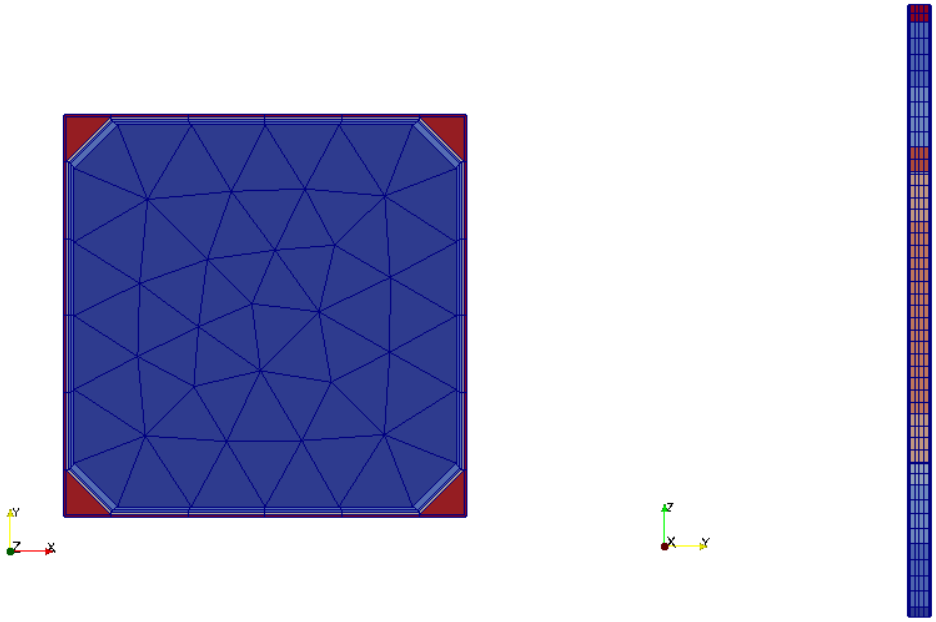

Fig. 3.3. Heterogeneous configuration and side view of block assignment.

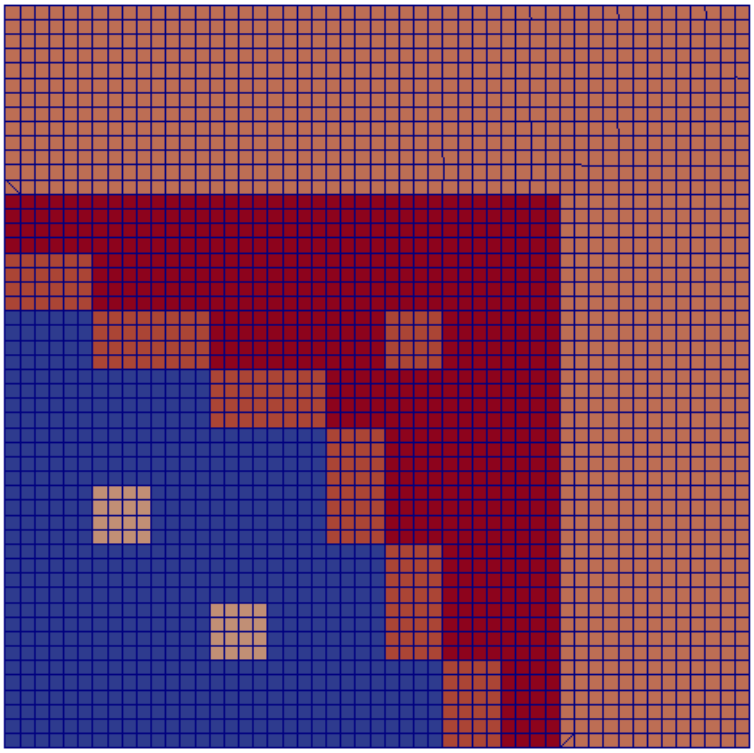

Fig. 3.4. Top down view of mesh for the *full* homogenization model of the minimum critical core.

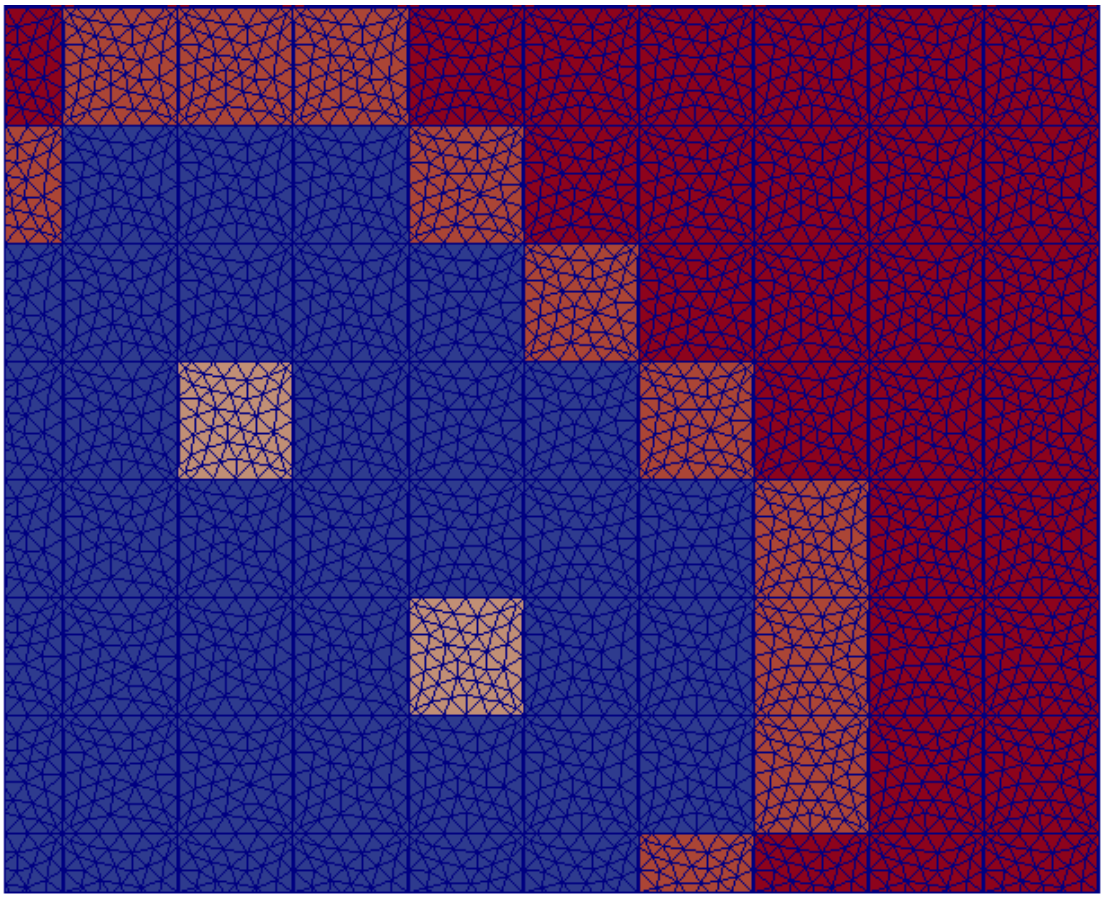

Fig. 3.5. Top down one-quarter view of mesh of *full* homogenization with explicit channels for minimum critical core.

3.3.4 Minimum Critical Core Model

The minimum critical core configuration (Fig. 2.1) was built to the various radial homogenization schemes and axially partitioned identically to the standard element models. Void boundary conditions were applied on all exterior sides of the models. Steady state calculations using the diffusion and P_N solver within MAMMOTH were completed to quantify eigenvalues, temperature coefficients, and leakage rates. Figure 3.4 shows a one-quarter top view of the meshed core with *full* homogenization. Only first order hexagonal elements are used in this core configuration. Fig. 3.5 shows a one-quarter top view of the meshed core with full homogenization with explicit channels. First order hexagonal and wedge elements are used in this configuration.

The temperature feedback for the full core is based on results from the adiabatic model evaluated at the end of the time-step and not directly included in the residual evaluation, essentially using an operator splitting approach (loose/weak coupling). Only the model with the full homogenization has been, in addition, evaluated with a strongly coupled system (the temperature is evaluated during the residual evaluation). Figure 3.6 shows a one-quarter top down view of the radial mesh for the full homogenized 159 Core. Only first order hexagonal elements are used in this core configuration. Figure 3.7 shows a one-quarter, top down view of the full homogenized with channels radial mesh for the 159-element core. First order hexagonal and wedge elements are used in this configuration.

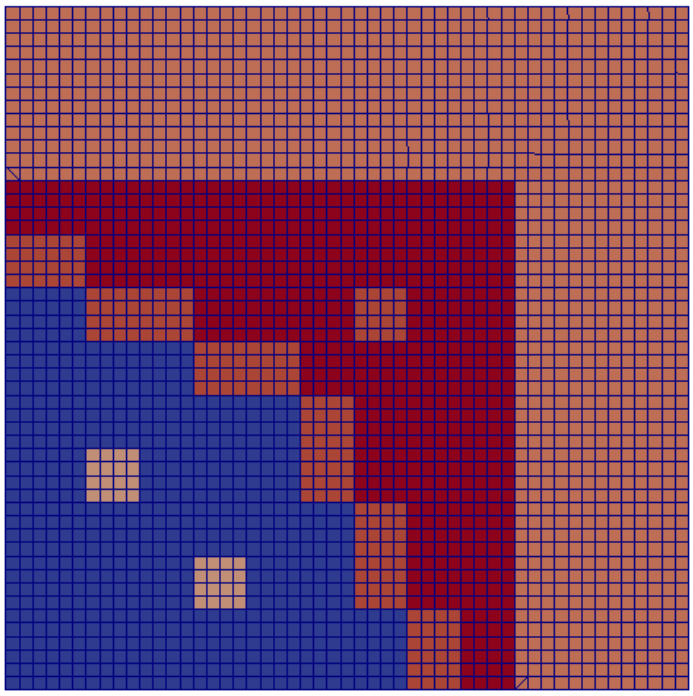

Fig. 3.6. Top down one-quarter view of mesh for the *full* homogenization for the 159-element core model.

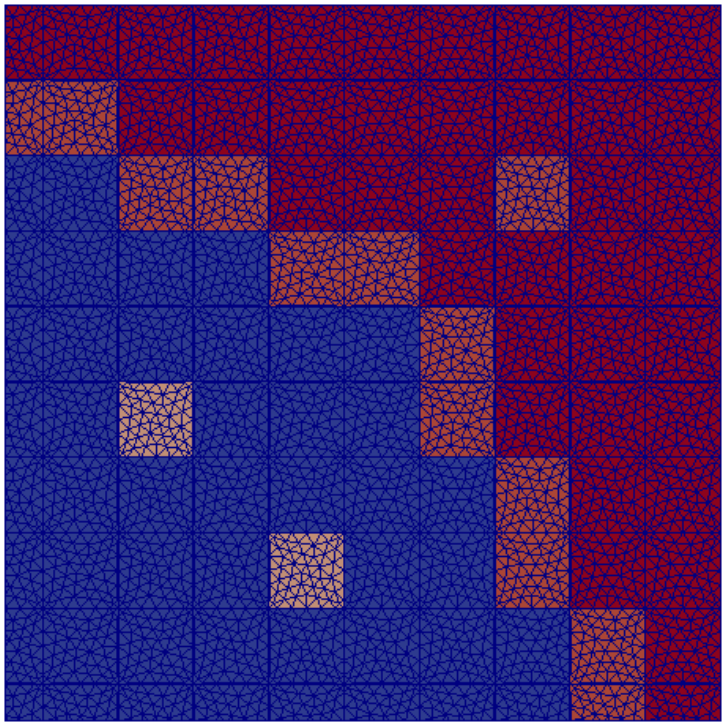

Fig. 3.7. Top down one-quarter view of mesh of *full with channels* for the 159-element core model.

4.0 RESULTS

For the majority of the results that are discussed in this report it is important to note that the value of k_{eff} enforces a balance between the production, absorption, and leakage of neutrons per Eq. 4.1.

$$k_{eff}=\frac{neutron\ production\ rate}{neutron\ leakage\ rate + neutron\ absorption\ rate} \quad (4.1)$$

In graphite reactors k_{eff} does not always accurately quantify what is taking place in the active core region. Since k_{eff} is an integral parameter, it includes all of the regions in the core, including reflectors. Therefore, even if the power distribution in the core is accurately predicted, the absorption in the graphite reflectors and, to a lesser extent, the neutron leakage can greatly affect the eigenvalue. This is also true for the temperature coefficient of reactivity, which essentially uses the difference in two core states (at different temperatures) as seen in the definition of the temperature derivative of reactivity (Eq. 4.2). The primary feedback mechanism in TREAT relies on neutron spectral shift, which is a change in the core neutron energy spectrum resulting from a change in temperature. As the graphite in the core heats up, the thermal Maxwellian distribution and hence the average energy of thermal neutrons within the core also increase. This spectral shift increases the leakage out of the active region and absorption in the reflector regions. The temperature coefficient of reactivity effectively combines these effects, and therefore can lead to inconclusive results with regard to the actual power in the active core region.

$$\frac{\partial \rho}{\partial T} = \frac{(k2-k1)}{k2\ k1}\frac{1}{(T2-T1)} \quad (4.2)$$

Hence, the distribution and magnitude of power are the figures of merit to accurately simulate TREAT transients. The eigenvalue, neutron leakage at the boundary, and the absorption in reflector regions are of interest when they affect the power distribution via the reflector effect (neutrons incoming to the active core region).

4.1 Homogeneous Infinite Medium Calculations

The results from the k_∞ calculations for the infinite homogeneous core are included in Table 4.1 and show very good agreement, within 10 pcm, compared to the MCNP-5 reference. Note that the value provided for MCNP-5 is the combined collision absorption and track-length estimator, whereas for Serpent 2 the results from the implicit estimator is provided. The Rattlesnake results for the various continuous finite element transport solvers (Diffusion, P_N, and S_N) produce the same solution. Because Rattlesnake cross sections were produced by Serpent 2, the corresponding eigenvalues are in very close agreement.

A simple transient case has been used to ensure that all of the transport solvers in Rattlesnake produce consistent transient solutions. The cross sections obtained from Serpent are employed in this simulation and the boron concentration in the homogenized domain is decreased in order to insert positive reactivity by a decrease in absorption, simulating control rod withdrawal. The results shown in Fig. 4.1 demonstrate that the three continuous finite element transport solvers yield the same result. In the reported percentage error in power, the S_2 solution is taken to be the reference calculation. The time integration used was a

first order backward Euler method. Both diffusion and P_N solutions show excellent agreement with the S_N solution, indicating consistency in cross section data and the approach used to create the cross sections.

Table 4.1. Eigenvalues for the Infinite Homogenized Model

Code	k_∞	% Difference [pcm]
MCNP-5 (col/abs/trk)	1.76256	Reference (∓4)
Serpent 2 (implicit)	1.76236	-9.1
Rattlesnake (Diff/P_1/S_2)	1.76237	-8.7

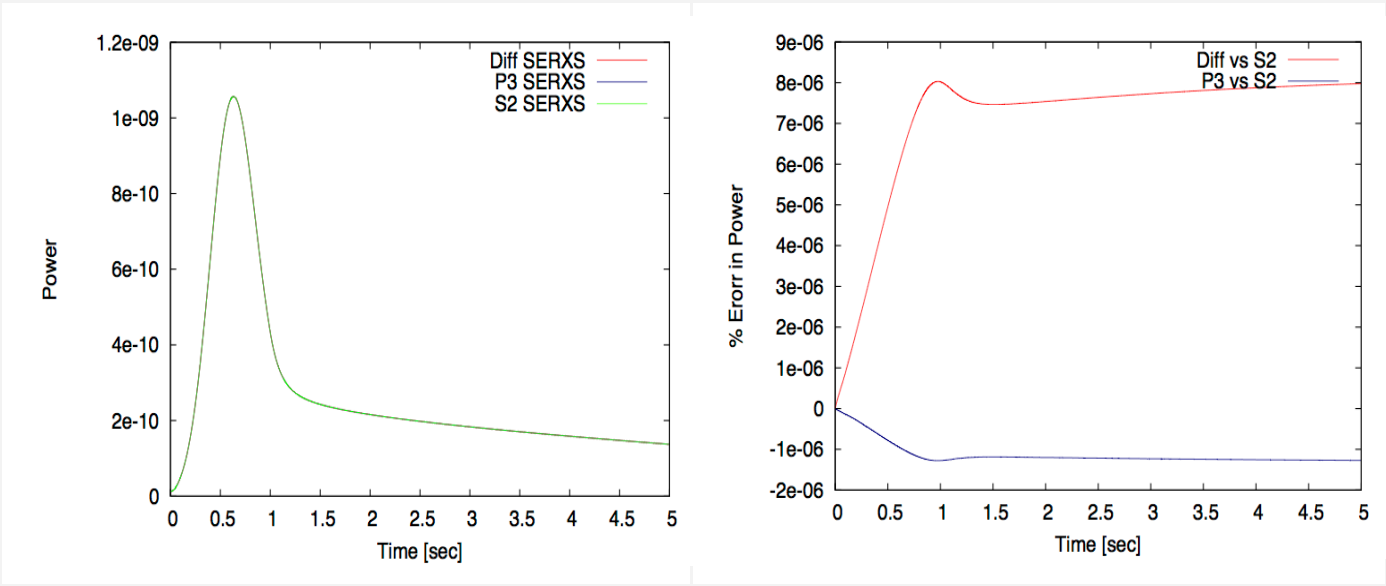

Fig. 4.1. Solver consistency test in a homogeneous media with Serpent cross sections (SERXS) prepared for diffusion, P_N and S_N solvers. Power is shown on left, error or right.

Knowing that cross section methods are consistent does not ensure that the transient solution is correct. Hence, comparison of an infinite medium point kinetics solution to the time-dependent transport solver in Rattlesnake is needed. Thus, transient calculations were performed for an infinite media mesh for comparison against a point kinetics solution using MPCA [24] using specified one-group cross sections and six delayed neutron precursor groups. Reactivity additions of \$0.05, \$0.25, \$0.50, \$1.00 and \$1.25 were evaluated using both step and five second ramp changes, with a first order implicit Euler method for time differencing and found to be in excellent agreement. Result for the \$0.05 and \$1.25 reactivity cases are provided here. Figure 4.2 illustrates Rattlesnake results for the two reactivity increases for a step insertion. Figure 4.3 shows the results of the same reactivity values inserted linearly over a 5 second period (\$1.25 ramp plotted with a logarithmic y-axis). Figure 4.4 is provided to illustrate the difference between Rattlesnake and the point kinetics solution of MPCA for the five ramp cases. For all ramps, there is an increase in the difference between Rattlesnake and MPCA power predictions early in the transient up to a peak of less than 10^{-3}. This then rapidly drops to less that 10^{-4}. However, as the power

increases the error begins to increase for the two super prompt critical ramps after about 3 seconds. This is possibly a result of time steps being too large for the rate of change in power per step for the implicit Euler time differencing scheme. This suggests further study with a higher order differencing approach.

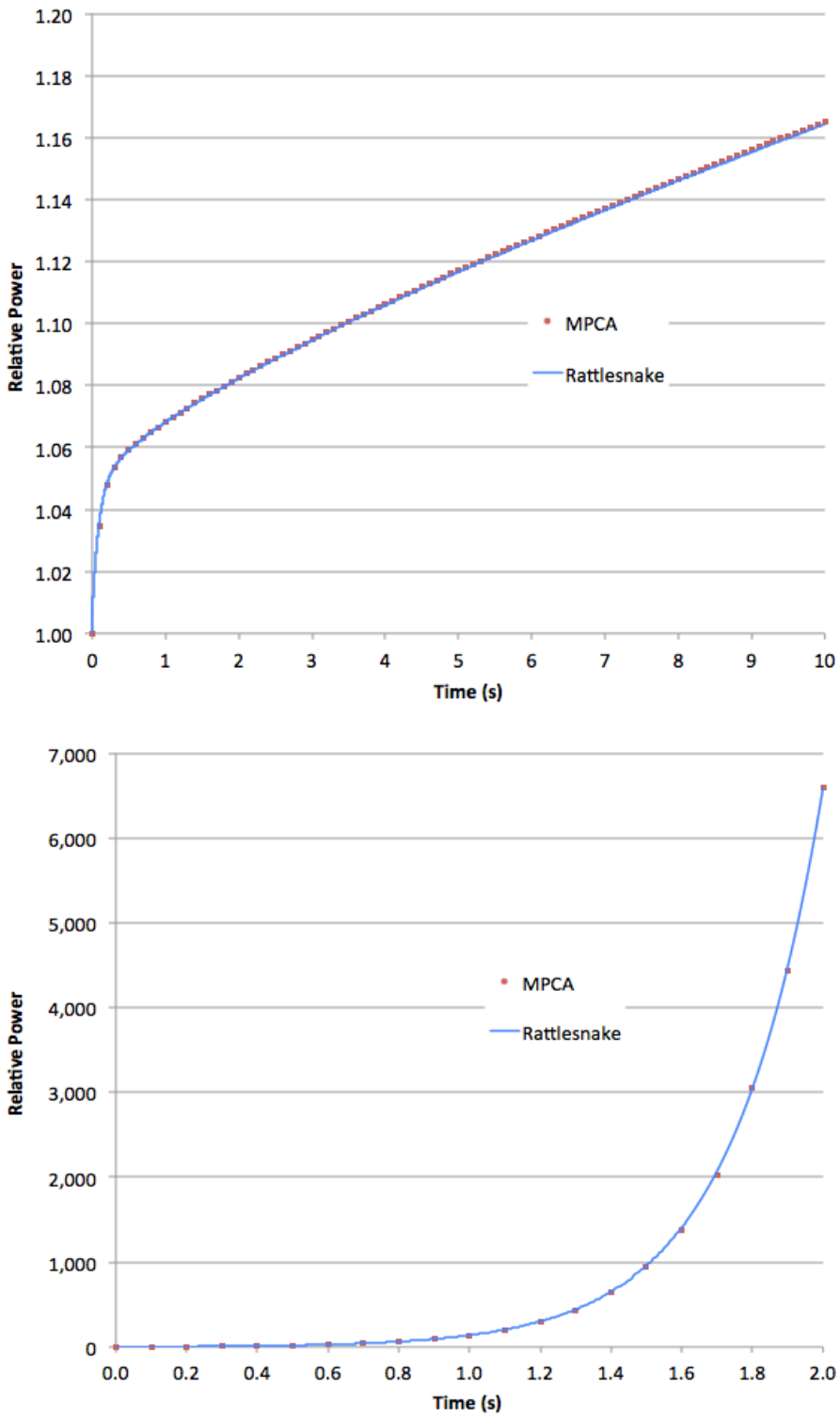

Fig. 4.2. Transient solver consistency with point kinetics solution and step reactivity increase in a homogeneous media ($0.05 on top, $1.25 on bottom).

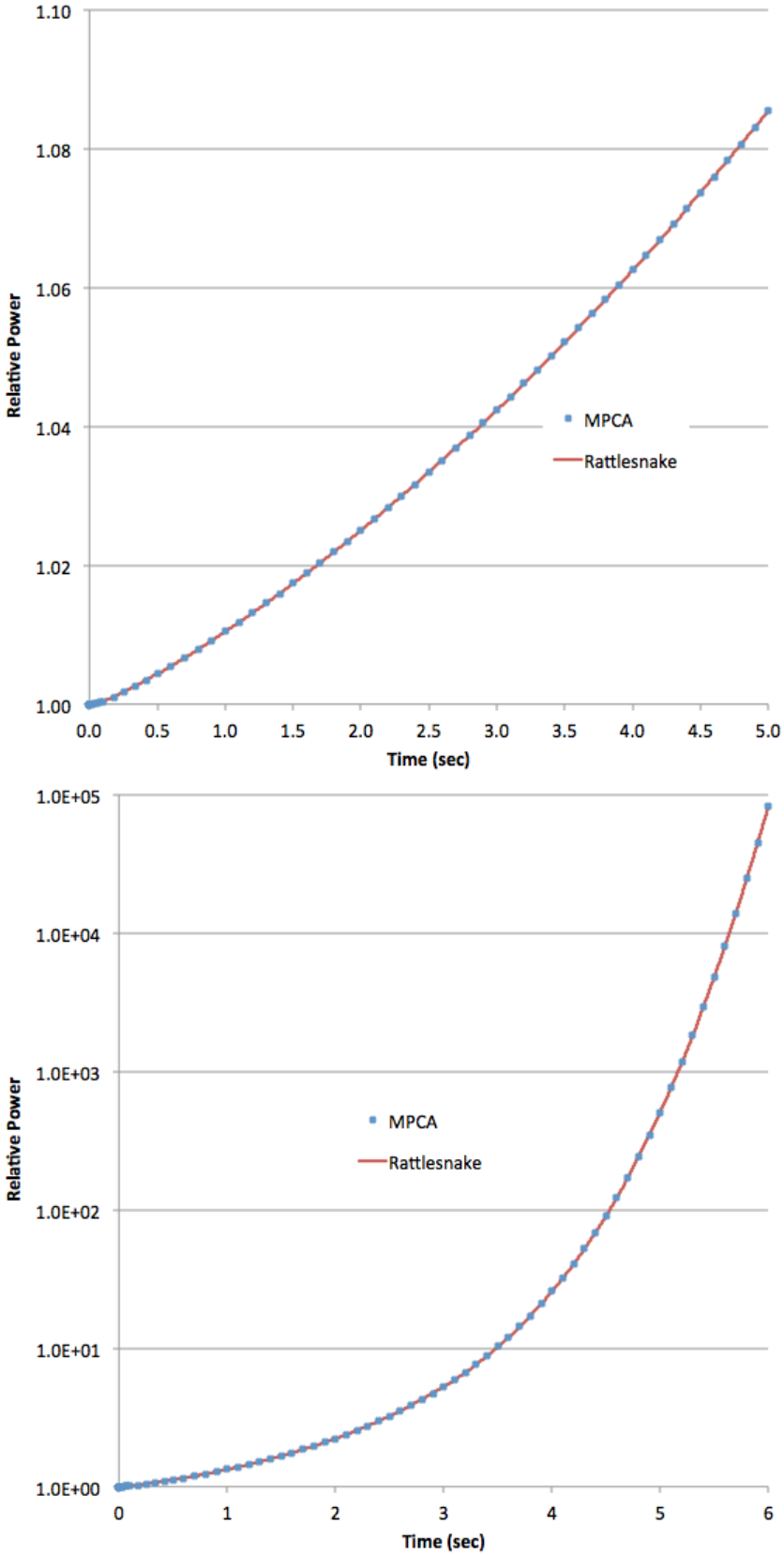

Fig. 4.3. Transient solver consistency with point kinetics solution for ramped reactivity increase in a homogeneous media ($0.01/sec on top, $0.25/sec on bottom).

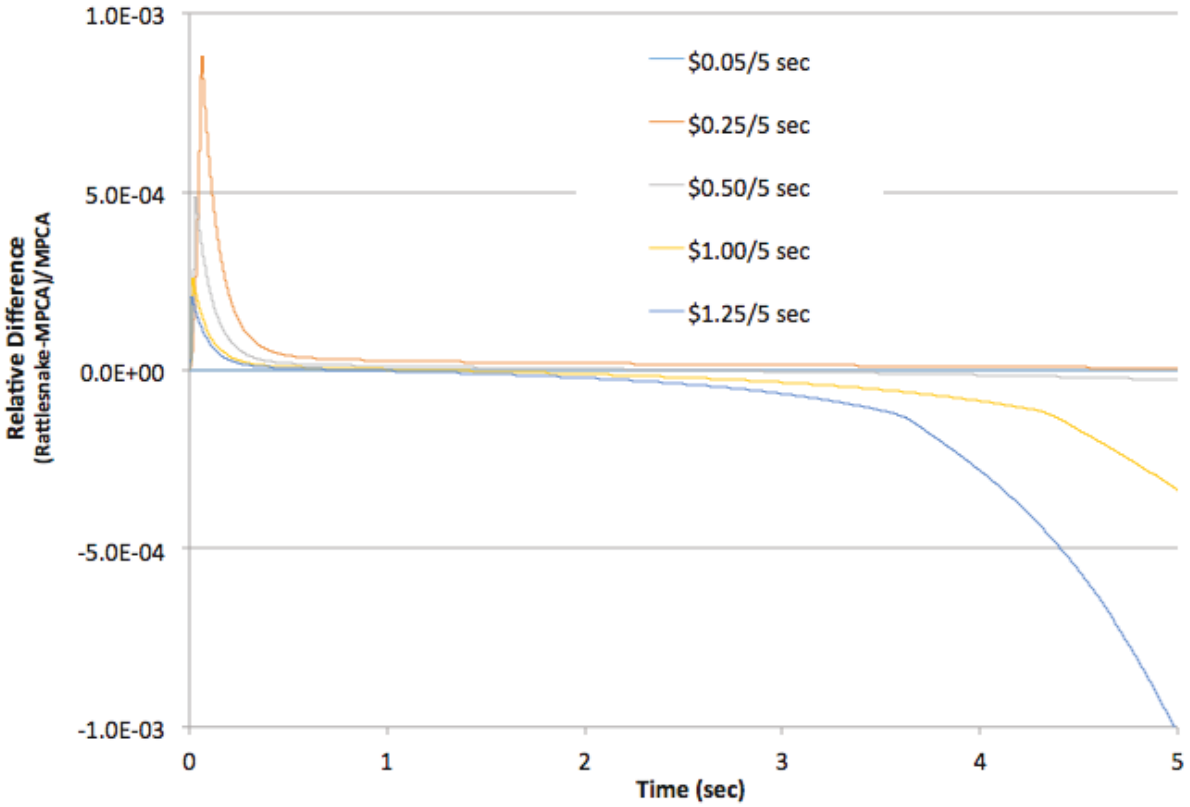

Fig. 4.4. Error relative to MPCA point kinetics solution for ramped reactivity change in a homogeneous media.

Finally, a set of more severe kinetics tests were evaluated using (1) alternating reactivities over a brief interval, based on a transient developed by Nobrega [25], and (2) a spiked reactivity insertion and withdrawal defined by Ganapol [24]. For the alternating reactivity, an initially critical medium is subjected to a reactivity insertion of $1/sec for 0.5 second, followed by an immediate reversal of -$1/sec for the next 0.5 second. The initial ramp of $1/sec for 0.5 second is repeated, then the total reactivity is maintained at $0.50 for the remainder of the calculation, out to 10 seconds. For the spiked case, a case was run for 5 seconds at which time the core reactivity was increased by $5; the transient was terminated 0.1 seconds later by a -$10 reactivity insertion. These transient were again evaluated comparing Rattlesnake to MPCA. Figure 4.5 shows the both codes track well together for the two extreme tests.

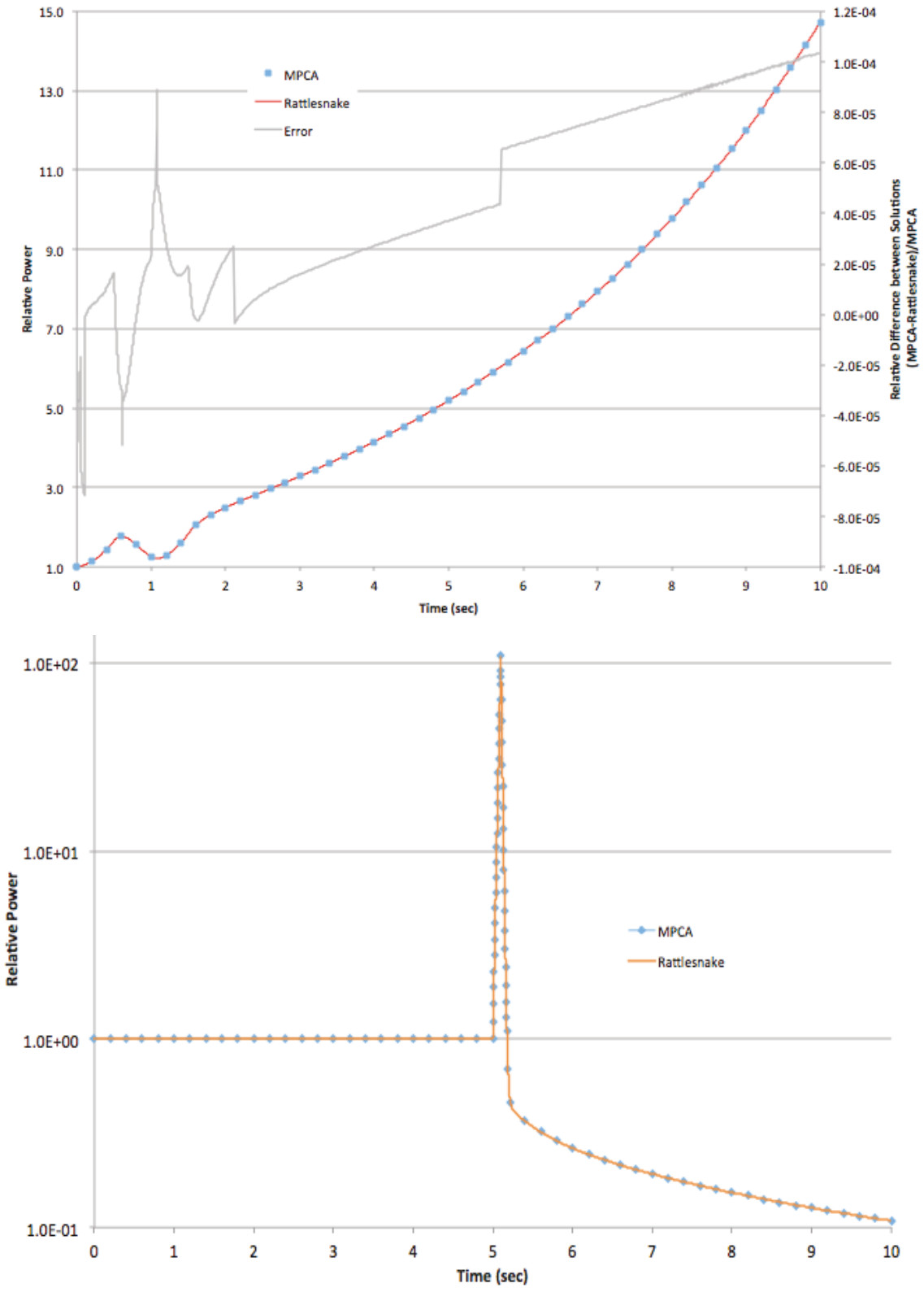

Fig. 4.5. Comparison of MPCA point kinetics solution to Rattlesnake for alternating (top) and spiked (bottom) reactivity in a homogeneous media.

4.2 Standard Fuel Element Calculations

In this portion of the study, calculations were first performed to assess the effect of various homogenization approaches with the Rattlesnake diffusion solver. The effect of these homogenization approaches on the calculation of a transient was then evaluated.

4.2.1 Steady-State Calculations for Standard Element

The Serpent 2 reference solutions for the standard fuel element steady state calculations are listed in Table 4.2. These calculations were performed with a fixed assembly power of 2000 W. The results show that 38.5% of all neutrons undergo capture at 300 K and that number increases to 40.7% at 800 K. The percentage of neutrons that leak at 300 K is 3.2% and the number increases to 3.6% at 800 K. Since the magnitude of the capture is an order larger than the leakage, once can conclude that the changes in the eigenvalue are primarily driven by the change in the fission rate (active region) and the capture rate in graphite (active and reflector region), and that leakage at the assembly boundary is a small component. The reported temperature coefficient is based on a fuel temperature increase and not a whole core temperature increase (isothermal case). The axial power density profile for the standard assembly is shown in Figure 4.6 for 300 and 800 K. One can observe the increase in the power near the center of the active core and a small depression near the reflectors at the higher temperature. This arises from the hardening of the neutron spectrum in the active core region and the subsequent increase in the capture rate and leakage out of the system, which reduces the number of thermal neutrons returning from the reflector regions.

Table 4.2. Serpent 2 results for the Type A element

Temp [K]	Serpent 2 k_{eff}	rel. error [pcm]	Serpent 2 TC $x10^{-4}$ [Δk/K]	Absorption Rate	Capture Rate	Leakage Rate
293.6	1.42202	1.5	-	1.0258E+14	4.0760E+13	3.3546E+12
400.0	1.4063	1.6	-0.739	1.0360E+14	4.1783E+13	3.5150E+12
600.0	1.37956	1.6	-0.689	1.0540E+14	4.3581E+13	3.7939E+12
800.0	1.35768	1.7	-0.584	1.0691E+14	4.5097E+13	4.0370E+12

Only a subset of the standard assembly Rattlesnake results for the various homogenizations is included in this report. More information is included in the cross section preparation report [20].

The diffusion solutions with full homogenization are shown in Table 4.3. The eigenvalues are significantly overestimated and worsen with increasing temperature. The temperature coefficient is within 5% of the reference and improves at higher temperatures. The inaccuracy of the eigenvalues and, consequently, the temperature coefficient is mainly driven by the under-prediction in the capture rate, which is ~2% lower than the reference. The predicted leakage is ~5% lower than Monte Carlo, but that is to be expected since the diffusion vacuum boundary condition will not be accurate and the fluxes away from the active core are not very accurate.

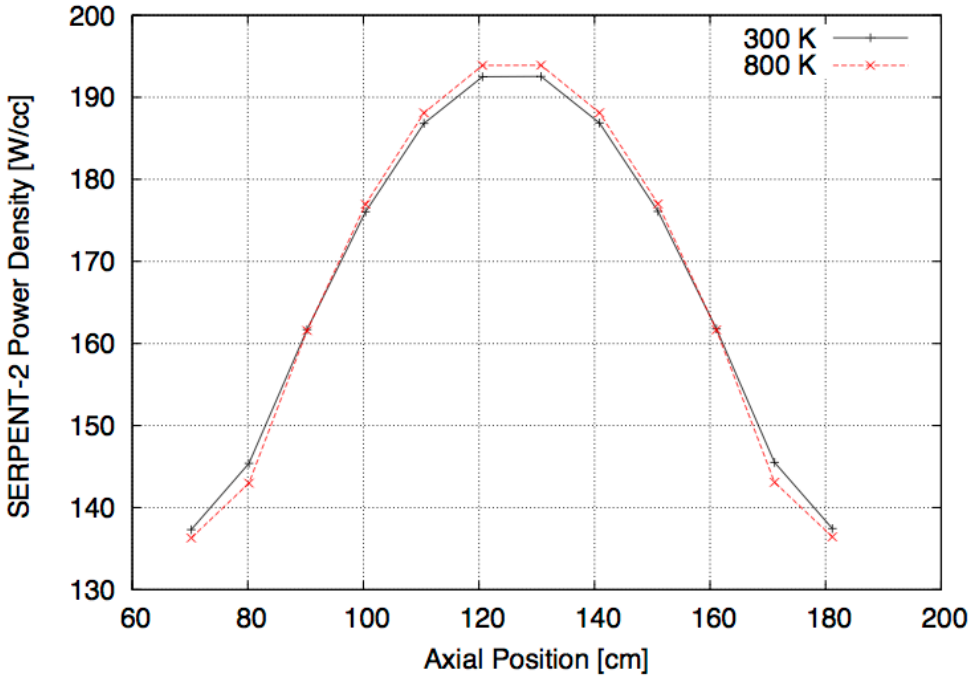

Fig. 4.6. Serpent-2 power density at 300 and 800 K (2000 W).

The results from the addition of the explicit channel to the *full homogenization* are included in Table 4.4. There is a great improvement in all of the parameters, except for the leakage, for which the difference has now increased to ~12%. The eigenvalues are now within 292 pcm of the reference and the maximum difference in the temperature coefficient is 1.35%. The difference in the capture rates has dropped to ~0.6%.

The diffusion solutions with the heterogeneous model also lead to an under-prediction of the k_{eff}, but within 118 pcm of the reference calculation at all temperatures. The difference in the temperature coefficient is similar in magnitude to that with the full homogenization with channels, but it shows opposite behavior with temperature. This model does produce worse capture and leakage rates than the full homogenized with channels.

The comparison of the calculated power densities to the Serpent-2 reference solution at 300 and 800 K are included in Figures 4.7 and 4.8, respectively. These comparisons show that the diffusion solutions with the majority of the homogenizations, except for the clad-air without explicit channels, yield very good agreement with the reference Monte Carlo. The difference in the power density is within 0.5% for the 300K and 0.9% for the 800K. Small incremental improvements can be observed as previously homogenized regions are separated. The best power density results are obtained with the heterogeneous model.

Table 4.3. Diffusion results for the Type A element with *Full* homogenization

Temp [K]	MAMMOTH k_{eff}	Error in k_{eff} [pcm]	Difference in TC [%]	Diff. in Abs. rate [%]	Diff. in Capture rate [%]	Diff. in Leakage rate [%]
293.6	1.43387	833.4	-	-0.70	-2.05	-4.34
400.0	1.41874	884.9	-5.31	-0.74	-2.12	-4.44
600.0	1.39291	967.8	-5.30	-0.82	-2.26	-4.45
800.0	1.37162	1026.5	-4.51	-0.88	-2.35	-4.31

Table 4.4. Diffusion results for the Type A element with *Full w channel* homogenization

Temp [K]	MAMMOTH k_{eff}	Error in k_{eff} [pcm]	Difference in TC [%]	Diff. in Abs. rate [%]	Diff. in Capture rate [%]	Diff. in Leakage rate [%]
293.6	1.41808	-277.3	-	-0.10	-0.56	12.70
400.0	1.40240	-277.5	0.08	-0.12	-0.58	12.52
600.0	1.37582	-271.5	0.19	-0.14	-0.61	12.30
800.0	1.35371	-292.1	1.35	-0.15	-0.63	12.65

Table 4.5. Diffusion results for the type A element with heterogeneous homogenization

Temp [K]	MAMMOTH k_{eff}	Error in k_{eff} [pcm]	Difference in TC [%]	Diff. in Abs. rate [%]	Diff. in Capture rate [%]	Diff. in Leakage rate [%]
293.6	1.42048	-108.1	-	-0.38	-1.24	14.80
400.0	1.40464	-118.3	1.04	-0.39	-1.26	15.09
600.0	1.37802	-111.8	-0.23	-0.43	-1.31	14.96
800.0	1.35615	-112.4	0.15	-0.45	-1.34	14.93

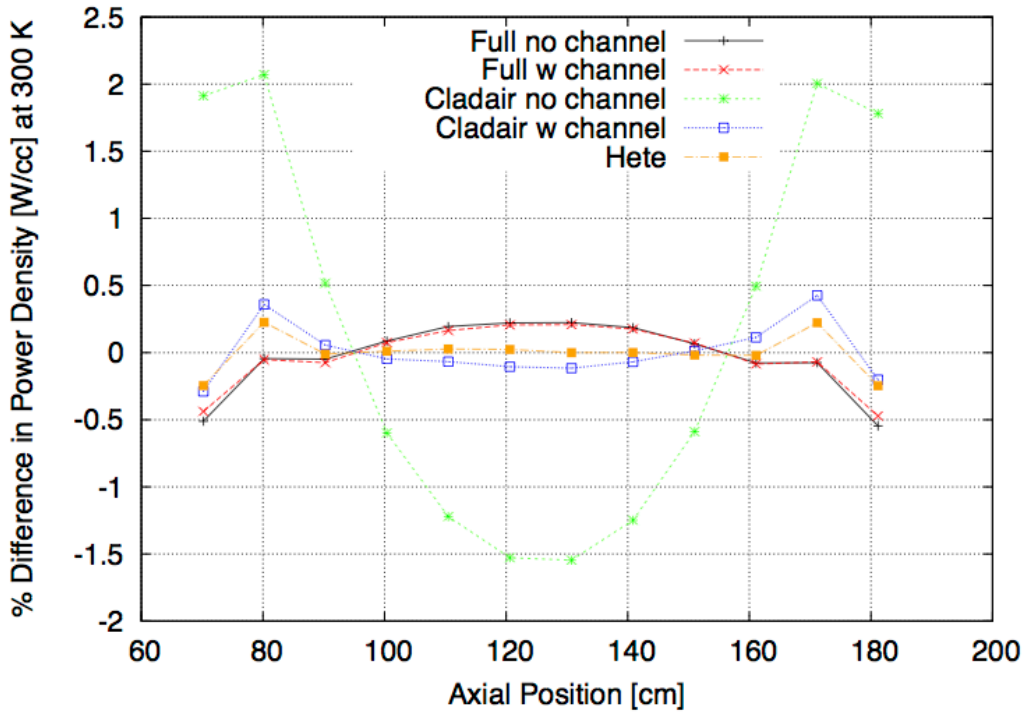

Fig. 4.7. Percent difference in the power density calculated with Rattlesnake diffusion versus Serpent-2 at 300 K.

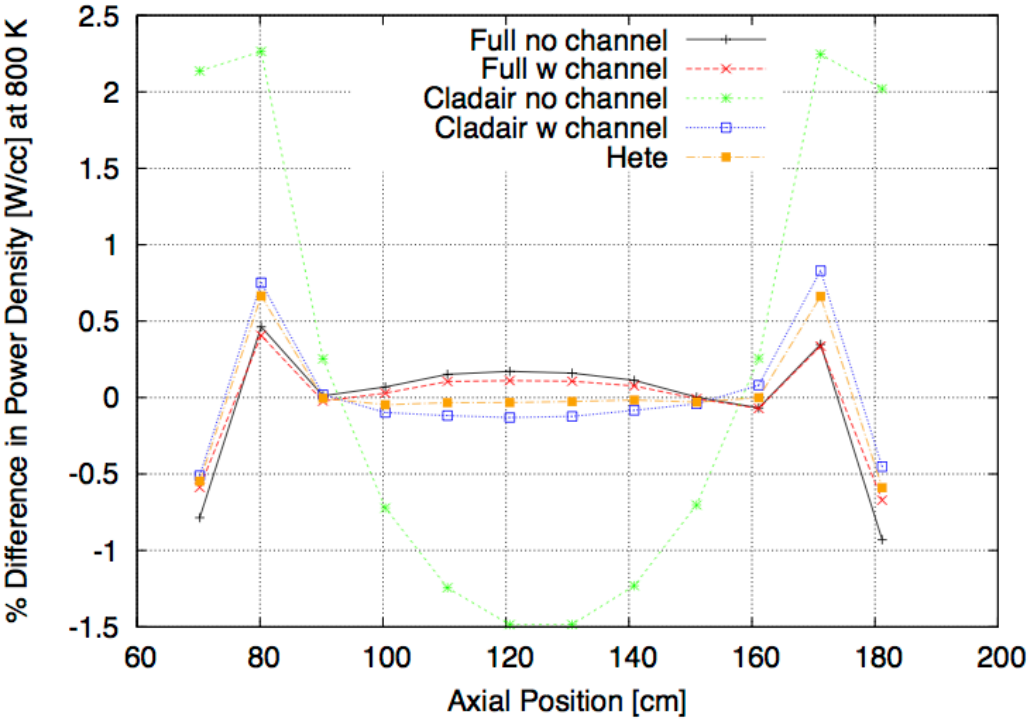

Fig. 4.8. Percent difference in the power density calculated with Rattlesnake diffusion versus Serpent-2 at 800 K.

4.2.2 Transient Calculations for Standard Element

The three homogenized models discussed in the steady state analysis are included the standard fuel assembly transient analysis. This transient corresponds to a 1.55% Δk reactivity insertion used in small core test 15 described earlier. All of the results included in this section are based on the solution to a strongly coupled system. The standard fuel element transient power is shown in Fig. 4.9. The power peak prediction is substantially different (25%) depending on the cross section homogenization approach used. The steady state analysis showed that the *full* homogenization model under-predicted the capture rate compared to the rest of the models, thus yielding the highest power peak. The two models with explicit channels are closer together, but the peak is a bit shifted. The integral powers are included in Fig. 4.10 and are consistent with the instantaneous transient power results, with the fully homogenized model showing higher integral powers. The average fuel temperature rise in the core shown in Fig. 4.11 indicates that the heat source for the thermal models is not completely consistent. The power deposited initially by the models with explicit channels appears to match closely for the first 1.3 seconds, after which they diverge. This can be attributed to differences in the models and it is manifested through the temperature coefficient (TC) of reactivity. The heterogeneous model has higher values of the TC below 400 K (roughly 1%), but this changes after 400K, where the TC value drops 0.5% below the value from the full homogenized model with channels.

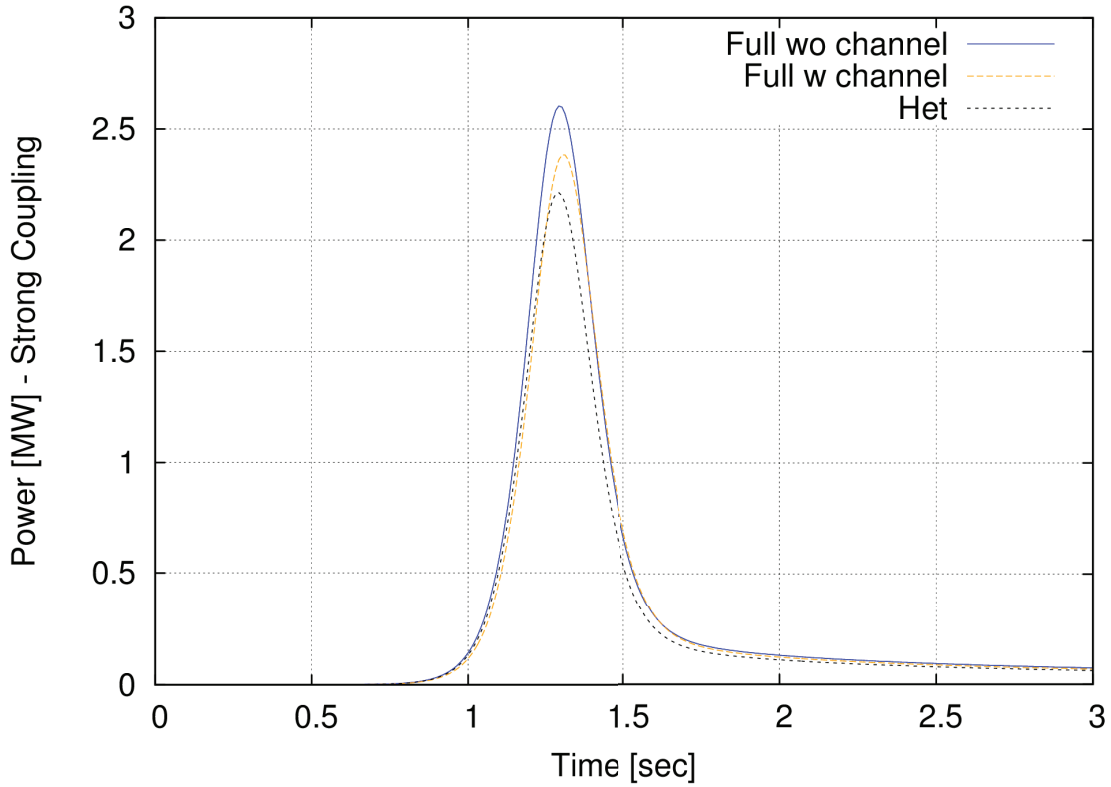

Fig. 4.9. Single Type A element power for the 1.55% Δk transient with the diffusion solver and the various homogenization methods.

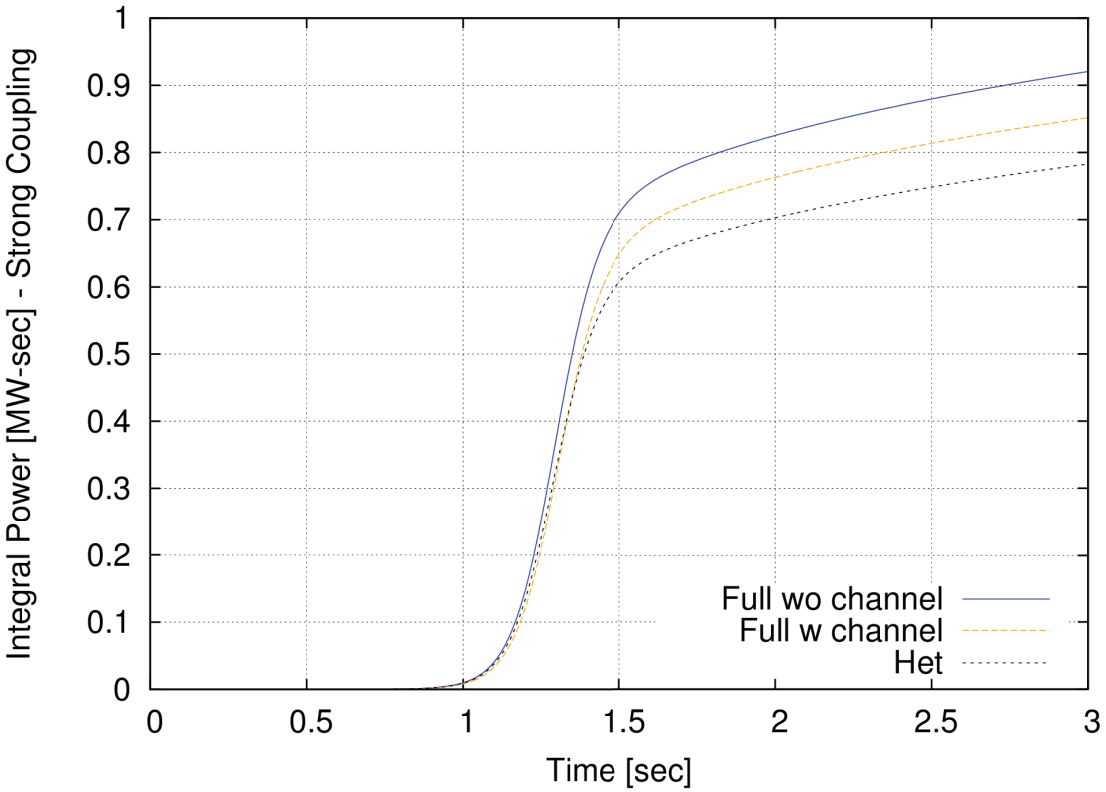

Fig. 4.10. Integral element power for the 1.55% Δk transient with the diffusion solver and the various homogenization methods.

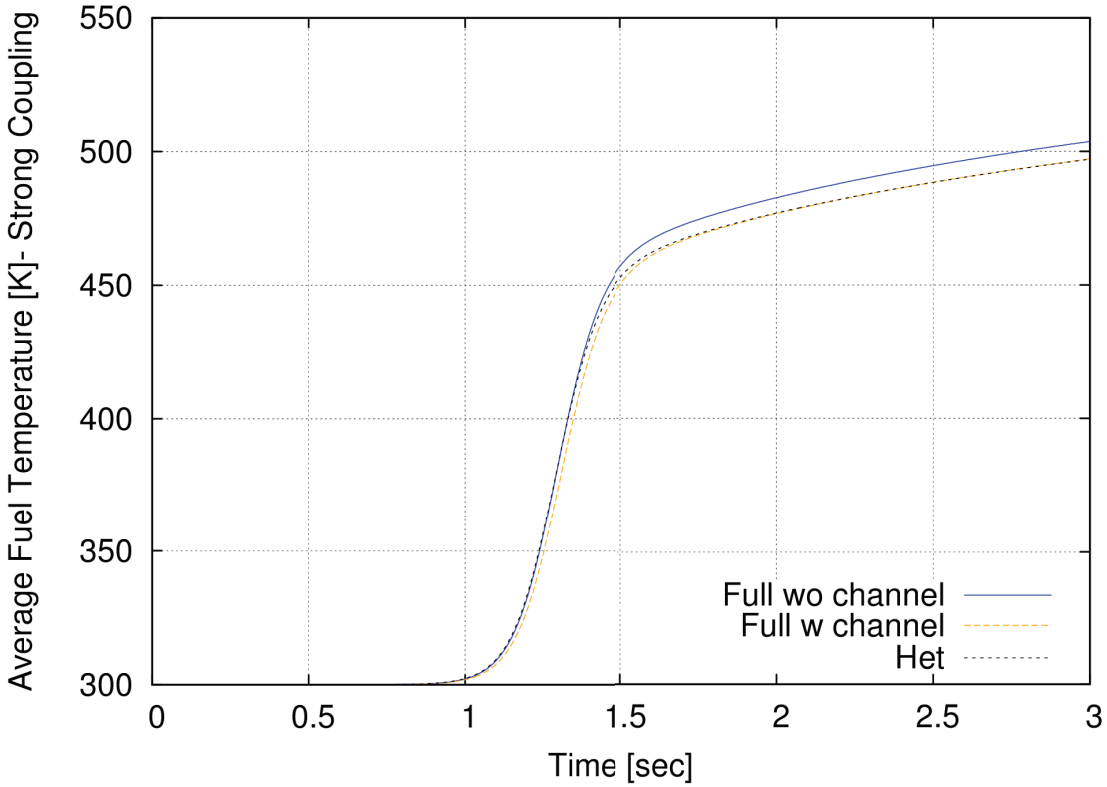

Fig. 4.11. Average fuel temperature for the 1.55% Δk transient with the diffusion solver and the various homogenization methods.

4.2.3 Observations on Homogenization Approximations for Standard Element

The diffusion solver predicts with high accuracy (<1%) the power distribution in the standard assembly at both low and high temperatures. The introduction of the explicit channel in the full homogenization improves the overall core absorption rates by improving the neutron streaming that takes place in the air channels. This is consistent with the results from the heterogeneous model. The transients show that the models with the explicit channels behave similarly with differences that are mainly driven by the disparity in the temperature coefficients (cross sections). The *full homogenized* model with explicit channels should produce an acceptable result for transient simulations, but a high-resolution transport simulation is desirable to determine the optimal diffusion model.

4.3 Full Core calculations

For calculations of the full TREAT core, two configurations were evaluated, as discussed in Section 2.3. The minimum critical core configuration was used to assess and validate MAMMOTH steady state calculations relative to measured data. Both homogenization and transport solver evaluations were performed. For transient calculations, the 1.55% Δk reactivity insertion of TREAT small core test 15 was simulated and used to assess various feedback coupling mechanisms.

4.3.1 Minimum Critical Core Configuration: Steady state calculations

Reference solutions for the minimum critical core configuration are shown in Table 4.7. The criticality condition is over-predicted with Serpent 2 by ~532 pcm. The results show the effects of the neutron spectrum hardening as a function of temperature with the consequent decrease in the eigenvalue and increase in the leakage. The temperature coefficients are significantly larger than those for the element, which is caused by the presence of additional moderator in the full core. The leakage has increased from the range of 3.5% in the element calculations to 8-9% for the core. This implies that the approximate radial leakage of the core is 5%.

Table 4.7. Serpent 2 results for the Minimum Critical Core

Temp [K]	Serpent 2 k_{eff}	rel. error [pcm]	Serpent 2 TC $x10^{-4}$ [Δk/K]	Neutron leakage [%]
293.6	1.00532	2.1	-	8.31
400	0.980262	2.1	-2.390	8.54
600	0.940395	2.2	-2.241	8.91
800	0.908709	2.2	-2.088	9.21

Diffusion solutions with the full homogenization approximation are shown in Table 4.8. The calculated eigenvalues and core leakage show a significant overestimation of the reference solution. In order to resolve this inconsistency a P_7 calculation was performed; the results of this calculation are given in Table 4.9. The P_7 results show the same trend for the eigenvalue, which indicates that the homogenized cross

sections are likely to be the problem rather than the order to of the transport solution. The temperature coefficients are consistent between the two calculations and with the element calculation, with an approximate difference of 5%. It was found that the error in the reaction rates for fission and absorption were -1.69% and -3.97%, respectively. Although these errors are relatively small compared to the leakage, their magnitudes are an order larger than that of the leakage (10^{14} for fission and absorptions vs 10^{13} for leakage) and are, as seen in the standard assembly models, the driving force for the error in the eigenvalue.

Table 4.8. Diffusion results for the Minimum Critical Core with *Full* homogenization

Temp [K]	MAMMOTH k_{eff}	Error in k_{eff} [pcm]	MAMMOTH TC * 10^-4	Difference in TC [%]	Neutron leakage [%]	Diff. in Neutron Leakage [%]
293.6	1.019275	1395.5	-	-	11.77	41.54
400	0.995462	1520.1	-2.273	-4.90	12.09	41.50
600	0.957642	1724.7	-2.134	-4.77	12.60	41.48
800	0.927643	1893.4	-1.990	-4.69	13.03	41.54

Table 4.9. P_7 results for the Minimum Critical Core with *Full* homogenization

Temp [K]	MAMMOTH k_{eff}	Error in k_{eff} [pcm]	MAMMOTH TC * 10^-4	Difference in TC [%]	Neutron leakage [%]	Diff. in Neutron Leakage [%]
293.6	1.021921	1660.1	-	-	10.28	23.60
400	0.997997	1773.5	-2.283	-4.48	10.56	23.59
600	0.959893	1949.8	-2.147	-4.19	11.02	23.67
800	0.929759	2105.0	-2.00	-4.21	11.39	23.73

Table 4.10 provides the results of a diffusion solution for the full homogenization with explicit channels, i.e. separating the fuel elements from the inter-element gaps and coolant channels. Unfortunately, the accuracy of the solution is sensitive to the values of the diffusion coefficient in the air channel. These were artificially adjusted to improve the power distribution. For the 293.6 K test case, the calculated fission and absorption rates under-predict the reference solution by 0.063% and 4.67%, respectively. This implies that the error in the total absorption rate cancels the error in the leakage rate, thus leading to improved eigenvalues, which are now within 200 pcm of the reference Monte Carlo. Figure 4.12 shows that the axially integrated power distributions in the core are within $\pm$0.55% of the reference. Additionally, the difference in the temperature coefficients is reduced to 1.55%. The main drawback of this approach is a significant overprediction of the leakage rate, which may have significant effects on transient simulations.

Table 4.10. Diffusion results for the Minimum Critical Core with *Full* homogenization with channels

Temp [K]	MAMMOTH k_{eff}	Error in k_{eff} [pcm]	MAMMOTH TC * 10^-4	Difference in TC [%]	Neutron leakage [%]	Diff. in Neutron Leakage [%]
293.6	1.005746	42.6	-	-	12.55	50.93
400	0.981075	81.3	-2.353	-1.55	12.89	50.89
600	0.958988	134.6	-2.211	-1.34	13.44	50.93
800	0.910500	179.1	-2.061	-1.29	13.90	50.96

The general shape of the error distribution in Fig. 4.12 can be attributed to cross-section preparation. The cross sections originate from a Serpent 2 full core calculation. In this model, the standard element cross sections produced are a representative average over all positions in the core. The manifestation of this averaging approach is the ring shape around the center of the core, which would likely be improved by adding more cross section regions for the standard element: central, next to reflectors, intermediate, next to control rod, etc. The root mean square variance for the core was calculated using Eq. 4.2.

$$\text{RMS} = \sqrt{(pd_1{}^2 + pd_2{}^2 + \ldots + pd_N{}^2)/N} \qquad (4.2)$$

Where N is the total number of elements with non-zero power and pd_N is power difference of element N.

In Fig. 4.13, RMS values for the power distribution are radially averaged for each axial region of the active core. The maximum error appears next to the top reflector. This large error can be attributed to the control rods, which are located in the top reflector. Like the other elements in the core, the control elements are fully homogenized up to the inter element gaps and coolant channels. This homogenization leads to the B_4C rods being smeared into the rest of the control element. Since no equivalence technique is currently used in the model, this smearing can lead to an over-prediction of the absorption reaction rate. Further work will expand to the detailed analysis of the control rod and neighboring assemblies.

0.000	0.000	0.000	-0.513	-0.375	-0.020	0.000	-0.016	-0.395	-0.539	0.000	0.000	0.000
0.000	0.000	-0.264	-0.319	-0.263	-0.061	0.143	-0.036	-0.254	-0.356	-0.362	0.000	0.000
0.000	-0.289	-0.200	-0.157	0.011	0.048	0.115	0.030	-0.023	-0.149	-0.239	-0.317	0.000
-0.498	-0.312	-0.128	0.019	0.061	0.172	0.193	0.153	0.062	0.027	-0.107	-0.303	-0.546
-0.368	-0.205	0.008	0.067	0.191	0.235	0.241	0.216	0.165	0.071	0.012	-0.246	-0.365
-0.021	-0.019	0.094	0.183	0.254	0.256	0.260	0.256	0.221	0.165	0.062	-0.036	-0.032
0.000	0.154	0.174	0.213	0.249	0.250	0.268	0.264	0.241	0.235	0.170	0.131	0.000
-0.002	0.007	0.106	0.197	0.250	0.261	0.279	0.246	0.230	0.185	0.086	-0.011	-0.018
-0.392	-0.216	0.036	0.118	0.199	0.252	0.275	0.251	0.222	0.091	0.017	-0.209	-0.377
-0.478	-0.322	-0.123	0.043	0.093	0.154	0.220	0.179	0.102	0.062	-0.101	-0.272	-0.462
0.000	-0.237	-0.180	-0.120	0.023	0.043	0.171	0.074	0.027	-0.090	-0.145	-0.278	0.000
0.000	0.000	-0.252	-0.274	-0.163	0.031	0.157	0.018	-0.183	-0.260	-0.234	0.000	0.000
0.000	0.000	0.000	-0.441	-0.319	0.031	0.000	0.014	-0.335	-0.423	0.000	0.000	0.000

RMS 0.227
Min -0.546
Max 0.279

Fig. 4.12. Full homogenized with channels minimum critical core configuration, at a uniform temperature of 293.6K, using the Rattlesnake diffusion solver.

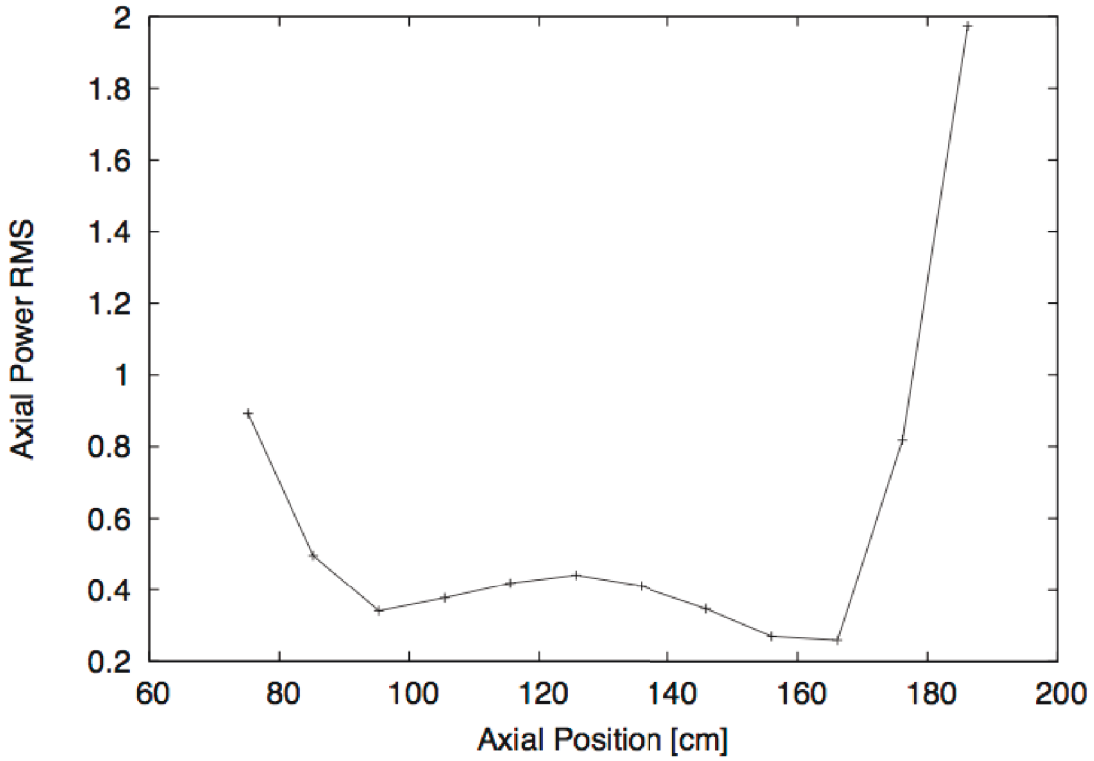

Fig. 4.13. RMS value of power difference as a function of axial position (measured from bottom of the core).

4.3.2 Small Core Test 15: Full Core Transient Calculations

The results from the 159 element core transient calculations are shown in Figs. 4.14 to 4.16. Only simulations of the *full homogenized* model (with and without explicit channels) are included in this section of the report, since work continues on building better models. The solution with strong coupling is included for comparison. With the Crank-Nicolson time integrator and the current time step set at 0.01 seconds the weakly coupled solution over-predicts the peak of the strongly coupled solution by 7%. The two radial homogenization approaches show a similar trend to that observed in the single assembly calculations with the fully homogenized model achieving a higher peak. The effect of the explicit channel has a smaller impact with the full core model with a difference in the peak of 5.1%, whereas in the assembly model the difference in the peak was 9.2%. This is confirmed with both the integral power and average fuel temperature in the core.

The peak power of 123.2 MW obtained in this simulation is significantly lower than that of the experiment, which is reported at 380 MW. The maximum temperature rise calculated for the core at 3 seconds is 140 K, and occurs at the core center. The temperature rise in location K-14 in the experiment was measured at 110 K [17]. Based on the radial distribution provided on the same report, the center assembly would be 30-40 degrees higher than location K-14, which is consistent with the model prediction. Figure 4.17 provides a qualitative comparison of the transient as computed by MAMMOTH and as provided in Fig. 30 of Ref 17. Although the peak powers are mismatched, the shape and timing of the computed transient are remarkably consistent with reported data.

There are a number of problems could lead to this lower prediction in peak power and include the kinetics and thermal data as well as the modeling assumptions. A sensitivity performed on the magnitude of the coefficient used in the adiabatic model is included in Figure 4.18. The results suggest that a reduction in the local energy available to raise the temperature leads to significant power increases. Since the time scale of heat transfer in graphite is pretty small, the redistribution of the heat within the core should have a significant impact on the power peak for this transient. The results also show that a shift in the power peak occurs due to the delay in the temperature feedback in the cases with lower coefficients. The experimental results (Figure 17) reveal that the peak power occurs later than in the MAMOTH prediction, which is indicative of a problem with the heat transfer model. Another set of runs used to determine the sensitivity to the magnitude of the reactivity insertion are shown in Figure 4.19. For these runs the CR is fully diluted at time 0.0 seconds, whereas in the previous runs the rods were diluted linearly from 0.0 to 0.08 seconds. This latest model includes temperature dependent coefficients for the adiabatic heat transfer model, which lead to a lower peak for the nominal case. The trend in the peak power is consistent with the experimental results from Figure 17, causing shorter times to reach the peak power peak and a larger magnitude of the peak. There could be other potential issues with the model. One possible cause, which was previously mentioned, is the poor prediction of the core leakage rate.

4.2.3 Observations on Full Core Transient Simulations

The results from the minimum critical study reinforce the insights developed from the standard assembly problem. The diffusion solution using the *full homogenized* model with explicit channels reproduces very well the reference Monte Carlo (< 50 pcm). Both the Monte Carlo and the deterministic models over predict the core critical state by ~600 pcm. The full homogenization approach under-predicts the core fission and capture rates. Adding the explicit channel improves both rates but increases the core leakage significantly, which could be one of the causes of the under-prediction of the peak power during the full core transient simulation. Future work with this transient will focus on improved neutronics and thermal modeling.

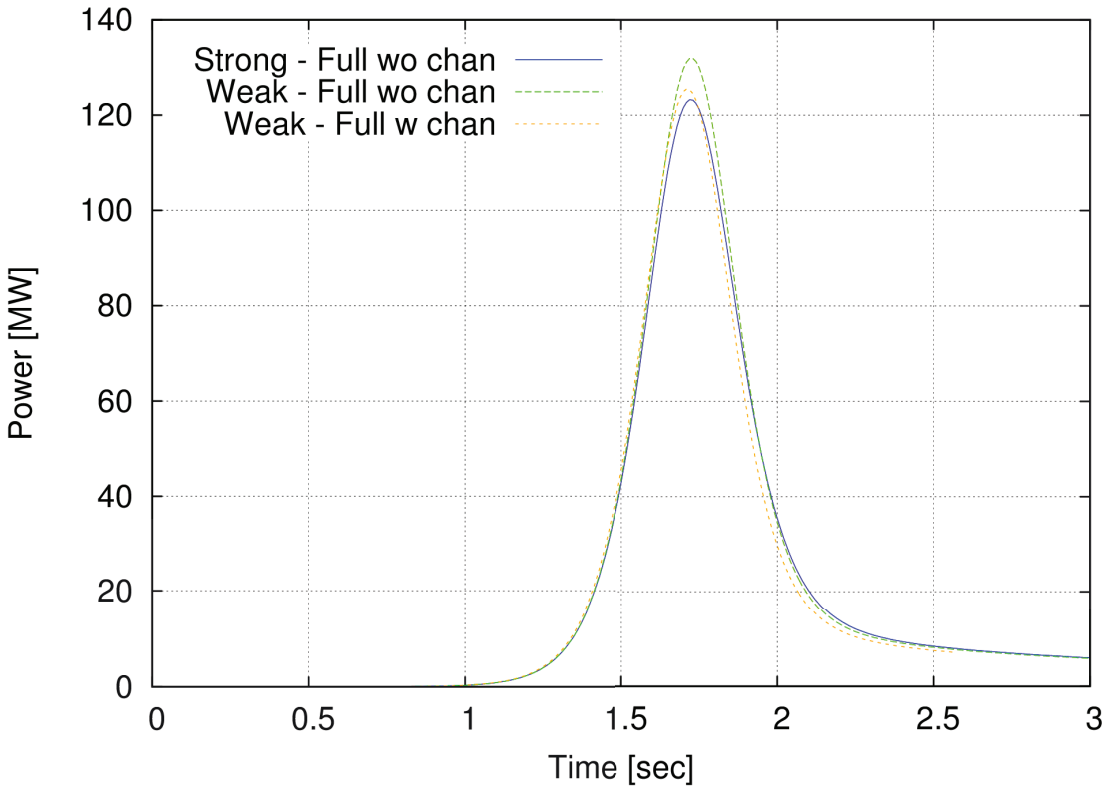

Fig. 4.14. Core power for the 1.55% Δk with a diffusion solution.

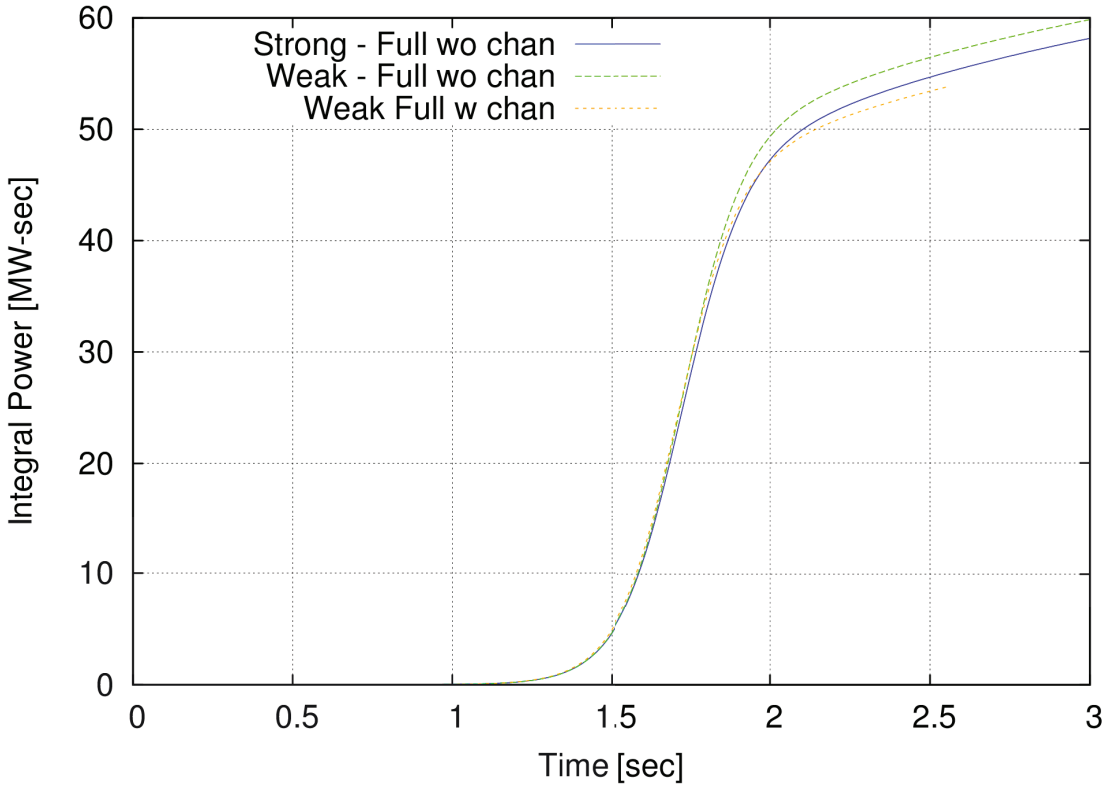

Fig. 4.15. Core integral power for the 1.55% Δk with a diffusion solution.

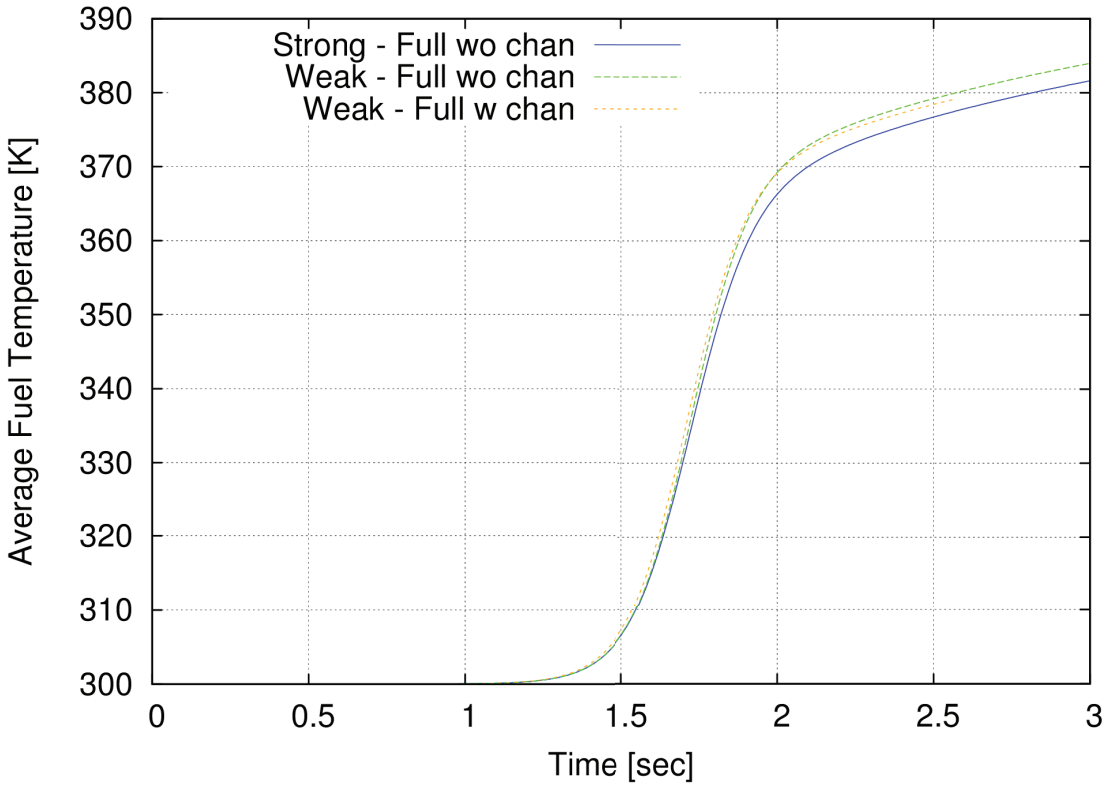

Fig. 4.16. Fuel average temperature for the 1.55% Δk with a diffusion solution.

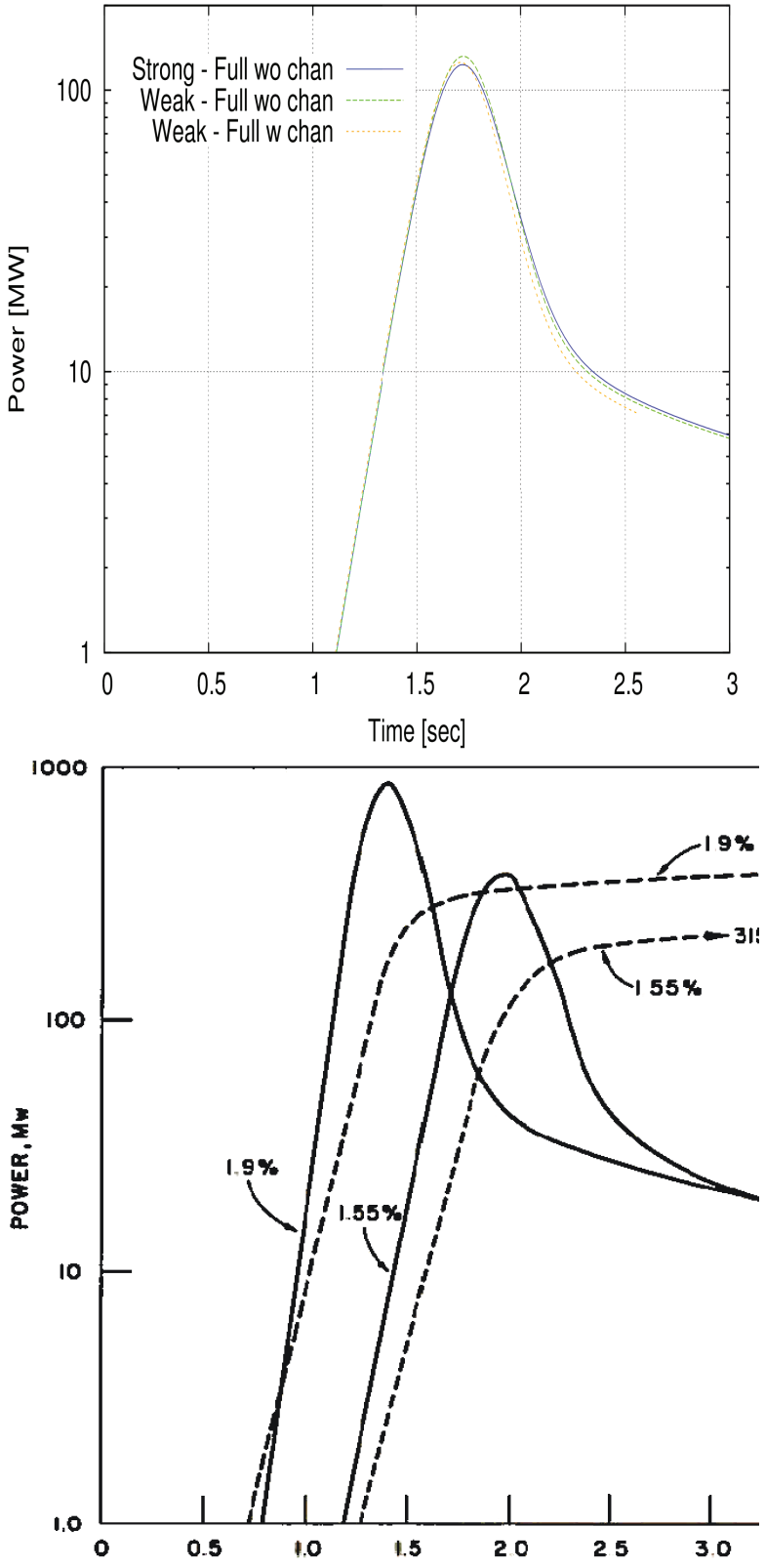

Fig. 4.17. Comparison of computed 1.55% Δk results (top) with log-power plot of the measured transient (bottom) [17].

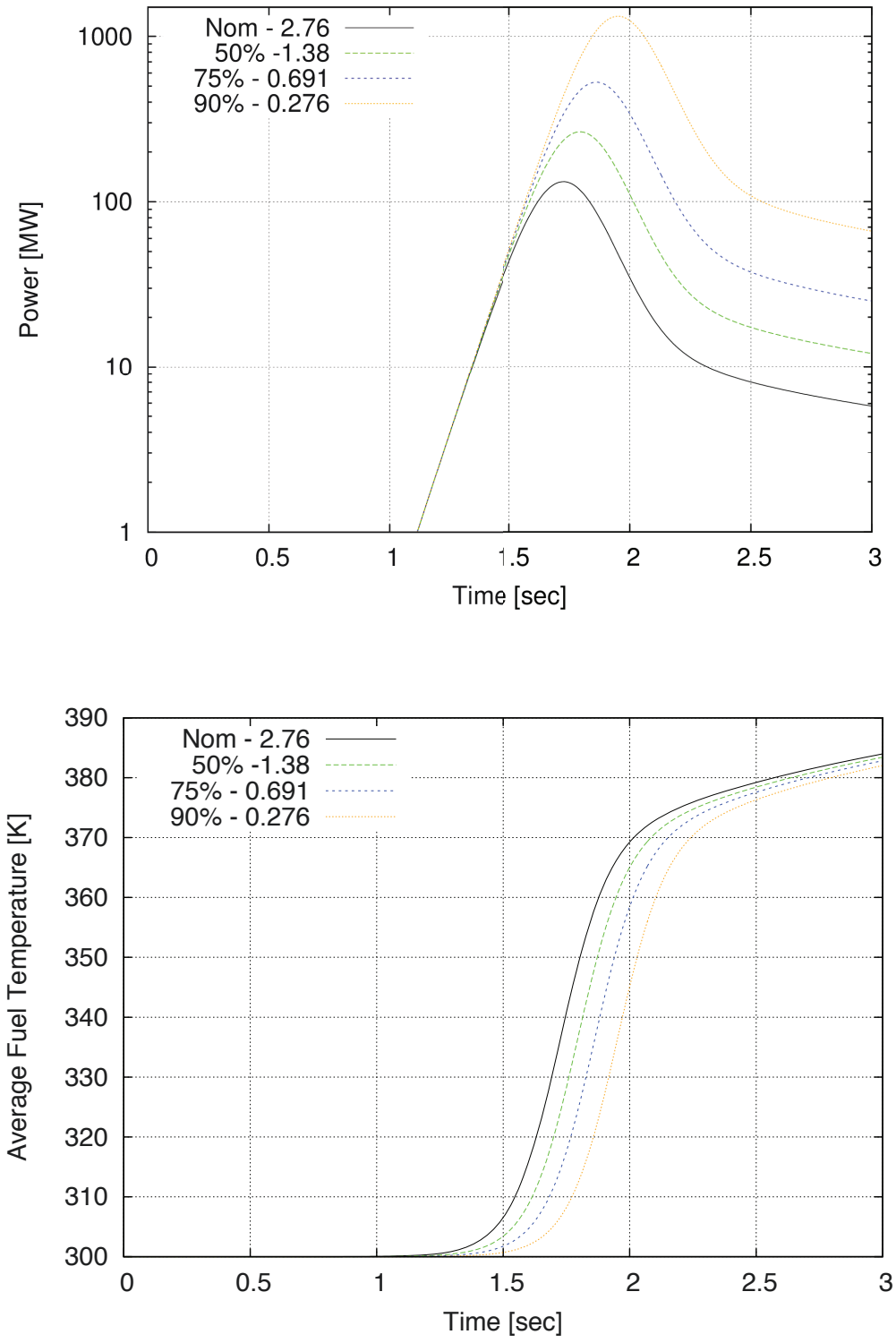

Fig. 4.18. Sensitivity of the power and average fuel temperature to the adiabatic model coefficient.

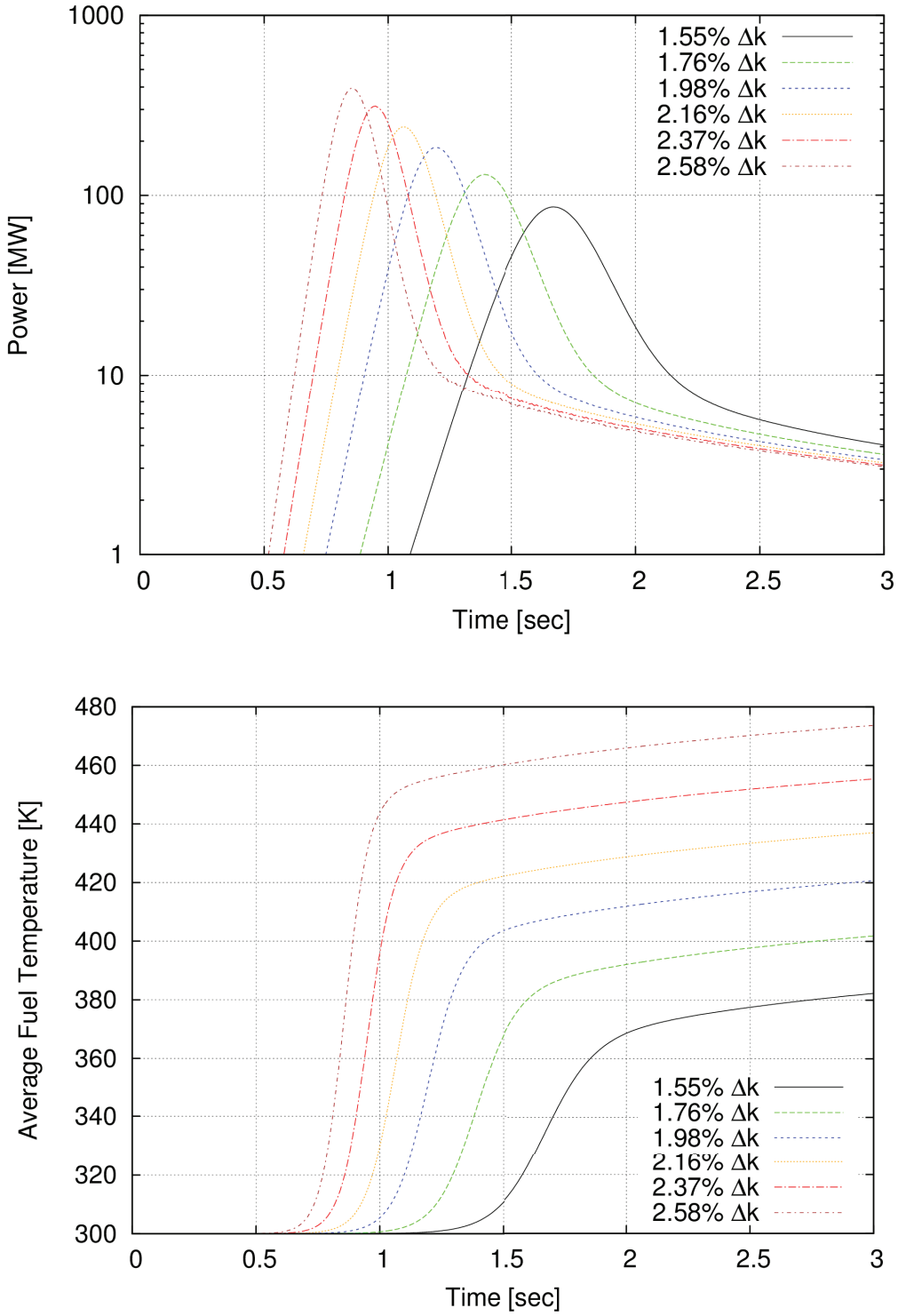

Fig. 4.19. Sensitivity of the power and average fuel temperature to the magnitude of the reactivity insertion.

5.0 SUMMARY

This work has focused on a fully coupled simulation of TREAT under transient conditions. While this capability has been successfully demonstrated here, significant work was necessary to validate the transport solution by comparing to a reference Monte Carlo solution using Serpent 2. Studies were performed for an infinite medium problem to ensure consistency with Serpent 2 and between the various solution options within Rattlesnake; Rattlesnake solvers all converged to the same solution. Point kinetics comparisons were also made to verify that Rattlesnake is properly solving the full time-dependent version of the transport equation for different reactivity insertions. Next, calculations were performed using an infinite lattice of standard TREAT fuel elements. This provided an opportunity to evaluate meshing, cross section axial cross section zoning requirements, the magnitude of error introduced by various homogenization schemes, and the relative performance of the various transport options for both steady state and transient conditions. The biggest challenge to fuel element modeling is the air/void regions between fuel regions. While voids themselves can cause issues in some methods, it appears that there is significant amount of leakage from the fuel region due to voids. Homogenization would tend to reduce this leakage, while the highly anisotropic behavior in these regions can be a challenge to explicit modeling.

The final stage of this work examined full core kinetics with thermal feedback based on the simulation of a set of measured experiments. While the work completed to date has not been able to reproduce the power transient measured for this core, the results are consistent and indicate that thermal feedback mechanisms may not be fully capturing the behavior of the core. At this point, it is not clear if this deficit results from cross sections or from thermal data. Work is ongoing to improve understanding of the coupled physics within this core.

6.0 FUTURE WORK

Based on the results of these studies, it is clear that additional work will be required to resolve some of the concerns identified. These will include the following issues.

- Because of uncertainties in the measurement data available, future work for analysis of this core configuration will focus on development of a detailed reference solution with minimal approximations, i.e., an S_N or high order P_N solution and minimal homogenization with a refined mesh. This will provide a reference solution for the transient for better evaluation of modeling approximations.

- This work showed that air channels between elements provide a challenge for diffusion solutions. There is a need to identify an improved method for calculation of appropriate diffusion coefficients. In addition, implementation of directional diffusion coefficients should be pursued.

- There also is a need to improve thermal modeling. Limited study of thermal modeling was performed in the current work. An improved adiabatic model with a temperature dependent temperature conversion coefficient will be developed. In addition, full solutions to the temperature field need to be evaluated to determine the range of applicability of the adiabatic model.

Beyond this configuration, future efforts will expand to larger cores with measured fuel experiments, to assess the ability of MAMMOTH to predict core-to-experiment coupling. Accurate simulation of coupling during a transient will be crucial for experiment multi-physics modeling.

7.0 REFERENCES

1. U.S. Department of Energy, "Mission Need Statement for the Resumption of Transient Fuel Testing ," U.S. DOE, December 3, 2010.
2. U.S. Department of Energy, "Resumption of Transient Testing Capability," April 15, 2013, http://energy.gov/ne/articles/resumption-transient-testing
3. G. A. FREUND, H. P. ISKENDARIAN, and D. OKRENT, "TREAT, a Pulsed Graphite-Moderated Reactor for Kinetics Experiments," Proc. 2nd United Nations Int. Conf. on the Peaceful Uses of Atomic Energy, Geneva, Switzerland, 10, 461-475 (1958).
4. F. N. GLEICHER, M. D. DEHART, J. ORTENSI, Y. WANG, A. L. ALBERTI and T. S. PALMER, "Evaluation of Multi-Physics Methods to Support Restart of the Transient Test Reactor," Trans. Am. Nucl. Soc., ANS Annual Meeting, San Antonio, Texas. June 7-11, 2015.
5. M. D. DEHART, F. N. GLEICHER, J. ORTENSI, A. L. ALBERTI and T. S. PALMER, "Multi-Physics Simulation of TREAT Kinetics using MAMMOTH," Accepted for publication, Trans. Am. Nucl. Soc., ANS Winter Meeting, Washington DC, November 8-12, 2015
6. R&D Magazine, "2014 R&D 100 Award Winners," Retrieved from http://www.rdmag.com/award-winners/2014/08/2014-r-d-100-award-winners (Aug 27, 2014)
7. D. GASTON, C. NEWMAN, G. HANSEN, and D. LEBRUN-GRAND'E, "MOOSE: A parallel computational framework for coupled systems of non-linear equations," Nucl. Eng. Design, 239, pp. 1768-1778 (2009).
8. F. N. GLEICHER, et. al. "The Coupling of the Neutron Transport Application RATTLESNAKE to the Fuels Performance Application BISON," International Conference on Reactor Physics (PHYSOR 2014), Kyoto, Japan, (May 2014).
9. Y. WANG. "Nonlinear Diffusion Acceleration for the Multigroup Transport Equation Discretized with S_N and Continuous FEM With Rattlesnake," Proceedings to the International Conference on Mathematics, Computational Methods & Reactor Physics (M&C 2013), Sun Valley, Idaho, USA (May 2013).
10. D. ANDRS, et al., "RELAP-7 Level 2 Milestone Report: Demonstration of a Steady State Single Phase PWR Simulation with RELAP-7," INL/EXT-12-25924 (May 2012).
11. R. L. WILLIAMSON, et al., "Multidimensional Multi-physics Simulation of Nuclear Fuel Behavior," Journal of Nuclear Materials, 423: 149–163, (2012).
12. J. D. HALES et al., "Advanced multiphysics coupling for LWR fuel performance analysis," Annals of Nuclear Energy, 84: 98-110, (2015).
13. M. ROSE, T DOWNAR and F.N. GLEICHER, "Redwing: a MOOSE application for coupling MPACT and BISON," Trans. Am. Nucl. Soc., ANS Annual Meeting, Anaheim, California, November 9-14, 2014
14. J. RAGUSA, and V.S. MAHADAVAN, "Consistent and accurate schemes for coupled neutronics thermal hydraulics reactor analysis," Nuclear Engineering and Design, 239: 566-579 (2009).
15. K. IVANOV and M. ACRAMOVA, "Challenges in coupled thermal-hydraulics and neutronics simulations for LWR safety analysis," Annals of Nuclear Energy, 34: 501-513 (2007).

16. D. OKRENT, C. E. DICKERMAN, J. GASIDLO, D. M. O'SHEA, D. F. SCHOEBERL, "The Reactor Kinetics of the Transient Reactor Test Facility (TREAT)," Argonne National Laboratory Report ANL-6174 (1960).
17. F. KIRN et al., "Reactor Physics Measurements in TREAT," ANL-6173, Argonne National Laboratory, October 1960.
18. J. LEPPANEN, "Serpent progress report 2012." VTT-R-00300-14, VTT Technical Research Centre of Finland, 2014.
19. G. MARLEAU, A. HEBER and R. ROY, "A User Guide for DRAGON Version5," Technical Report IGE–335, Ecole Polytechnique de Montreal, August 2015
20. J. ORTENSI et al., "Methodologies and Requirements for the Generation of Physics Data Inputs to MAMMOTH Transient Simulations in Support of the Transient Reactor Test Facility," INL/EXT-15-36265, (To be published, September 2015).
21. G. A. FREUND, P. ELIAS, D. R. MACFARLANE, J. D. GEIER and J. F. BOLAND, "Design Summary Report on the Transient Reactor Test Facility (TREAT)," ANL-6034 (1960).
22. R. MORRIS et al., "CUBIT 15.0 User Documentation," Sandia National Laboratory, https: //cubit.sandia.gov, (2015)
23. L.A. SCHOOF and V.R. YARBERRY, "Exodus II, A Finite Element Data Model," Sandia Technical Report SAND-92-2137-UC-705, Sandia National Laboratory, September 1994.
24. B. D. GANAPOL and P. PICCA, "A Modified Piecewise Constant Approximation for Solution to the Point Kinetics Equations," Accepted for publication, Trans. Am. Nucl. Soc., ANS Winter Meeting, Washington DC, November 8-12, 2015
25. J. A. W. NOBREGA, "A new Solution of the Point Kinetics Equations", Nuclear Science and Engineering, Vol. 46, p. 366-375, 1971.